KONDO TEMPERATURE OF A QUANTUM DOT

A Thesis
Presented to
The Academic Faculty

by

Seungjoo Nah

In Partial Fulfillment
of the Requirements for the Degree
Doctor of Philosophy in the
School of Physics

Georgia Institute of Technology
August 2011

KONDO TEMPERATURE OF A QUANTUM DOT

Approved by:

Professor Michael Pustilnik, Advisor
School of Physics
Georgia Institute of Technology

Professor Uzi Landman
School of Physics
Georgia Institute of Technology

Professor Markus Kindermann
School of Physics
Georgia Institute of Technology

Professor Michael Geller
Department of Physics and Astronomy
University of Georgia

Professor Vadym Apalkov
Department of Physics and Astronomy
Georgia State University

Professor Federico Bonneto
School of Matematics
Georgia Institute of Technology

Date Approved: 20 May 2011

To DOT,

of which sole existence is shaping up to be a center of my research

PREFACE

In a quantum dot system, a small number of electrons is confined in a finite region of space (the dot), which in turn is coupled via tunneling junctions to conducting leads. Transport characteristics of quantum dot systems exhibit a very strong dependence on the externally controlled parameters, such as gate potential, magnetic field, etc. This strong dependence forms the basis for the potential applications of quantum dot systems as nanoscale alternatives of the conventional field-effect transistors.

The tunneling between the dot and the leads induces transitions within the otherwise degenerate ground state manifold of the dot. These transitions give rise to the well-known many-body phenomenon - the Kondo effect, which dominates the properties of quantum dot systems at temperatures of the order of or below the so-called Kondo temperature.

In this thesis I first review the basic physics of the Kondo effect and its manifestations in quantum dot systems. Then I will concentrate on the dependence of the characteristic energy scale of the effect, the Kondo temperature, on the gate voltage, and show it to be very different from that in the conventional Anderson impurity model, commonly employed for the analysis of the experimental data. Some technical details are relegated to the Appendix.

ACKNOWLEDGEMENTS

I want to thank my committee who read my thesis and gave constructive comments, and my advisor, Prof. Michael Pustilnik, whose unprecedented teaching guided my research towards the right direction, for mentoring me in both physics and life, with lots of joyful conversation we had outside the Howey physics building, which I will miss a lot for long.

I cannot thank enough to my fellow graduate students, Alex Wiener, Adam Perkins, Ekapop Pairam, Yamato Matsuoka and Drs. Mike Sprinkle and Lee Miller of my classmates at Tech who not only inspired and stimulated me to be a keen physicist, but became friends of mine and shared their advice with me. I am very grateful to former graduate students at Georgia Tech, Drs. Dongju Lee, Jiil Choi, Seil Lee, Richard Inho Joh and Ed Greco for all their help. Drs. Kangjun Seo, Bokwon Yoon, and Joonho Bae encouraged me to finish my research at Tech. Jeremy Hicks, Mike DePalatis, Chris Malec, and Britt Torrence always helped shape my understanding in physics and electrical engineering by answering my questions.

I owe some of my knowledge and views of physics to Profs. Predrag Cvitanović, Roman Grigoriev, Kurt Wiesenfeld, David Finkelstein, Alex Kuzmich, and Uzi Landman and Dr. Wen Yang Ruan for their invaluable lectures and wisdom in physics. Prof. Andrew Zangwill, with his thoughtful advice, and a former chair, Prof. Mei-Yin Chou and her successor Prof. Paul Goldbart kept me pursuing my studies at Georgia Tech. Most of the writing of this thesis was done in Prof. Mike Shatz's Lab in part as well as in an anonymous location near Tech Square. Also, Prof. Harold Baranger at Duke university pointed out, in the 2011 APS march meeting in Dallas, what I hadn't paid attention to in my study until then.

Georgia Tech was a great place, with the warmth of Kevin Carter, Felicia Goolsby and Keith Garner to delve into and amuse myself doing physics upon wandering (and wondering) around campus in midtown Atlanta and sipping a variety of coffees in conversations with friends and colleagues. Most of all, the Yellow Jackets taught me the value of patience and hard working as well as gave me a fun time to follow them while conducting my research, through each season since 2006 and had me humming Ramblin' Wreck from Georgia Tech.

My thanks at last go to my wife and family and in-laws for their support and love.

TABLE OF CONTENTS

LIST OF TABLES

LIST OF FIGURES

SUMMARY

The low-energy properties of quantum dot systems are dominated by the Kondo effect. We study the dependence of the characteristic energy scale of the effect, the Kondo temperature T_K, on the gate voltage N_0, which controls the number of electrons in the strongly blockaded dot. We show that in order to obtain the correct functional form of $T_K(N_0)$, it is crucial to take into account the presence of many energy levels in the dot. The dependence turns out to be very different from that in the conventional single-level Anderson impurity model. Unlike in the latter, $T_K(N_0)$ cannot be characterized by a single parameter, such as the ratio of the tunneling-induced width of the energy levels in the dot and the charging energy.

CHAPTER I

KONDO EFFECT IN A SINGLE-ELECTRON TRANSISTOR

Advances in nanoscale fabrications and manifestations allow one to establish systems unapproachable in the past; single electron transistors (SET) and single molecule devices to name a few. Among a few interesting features of such devices, transport in nanostructures is of importance considering the weight of electronics and its application. A quantum dot is a common implementation of single electron transistors, and an ideal candidate for the study of transport in nanostructures [1, 2].

In quantum transport, a quantum dot (two-dimensionally confined region at the interface of two semiconducting layers, for instance, GaAs/AlGsAs in a lateral dot system) is capacitively connected via tunneling junctions to two massive conducting leads, the source and the drain [1, 2]. The differential conductance dI/dV of such device displays dependence on the external parameters such as temperature T, Zeeman energy due to a magnetic field $B = g\mu_B H$, and the source-drain bias V. The dependence of the differential conductance is well described by a formula in terms of the external parameters [3]

$$\frac{dI}{dV} \propto \frac{e^2}{h} \left[\ln \frac{\max\{T, eV, B\}}{T_K} \right]^{-2}, \tag{1.1}$$

where T_K is the characteristic energy scale in this transport. This anomalous behavior of the differential conductance was reported in various systems such as lateral semiconductor quantum dots [4, 5, 6, 7, 8, 9, 10], vertical quantum dots [11, 12], carbon nanotubes [13, 14], and single-molecule transistors [15, 16, 17], etc.

The logarithmic behavior of the transport coefficient over the external parameters has been known in condensed matter physics for a long time. When there is a magnetic

impurity in a host metal [18, 19], the resistivity of the system exhibits non-monotonic temperature dependence as well (the conventional Kondo effect) [20, 21, 22].

1.1 Conventional Kondo effect due to a magnetic impurity

The Kondo effect [23], the existence of the resistivity minimum at a certain non-zero temperature was discovered in the early 1930s [24]. From the experimental data, the contribution to the resistivity of the impurity in a metal was empirically given by [23, 25]

$$\delta\rho\,(T) \propto n_i \ln(\epsilon_F/T), \tag{1.2}$$

with the impurity concentration n_i and the Fermi energy ϵ_F. It is obvious that the impurity contribution Eq. (1.2) has a extremum to have a resistivity minimum, as the electron-phonon scattering contribution to the resistivity monotonically decreases when decreasing T. It should be mentioned again that the resistivity minimum develops only when the impurity atoms are magnetic [23]. The proportionality $\delta\rho \propto n_i$ has been verified down to the lowest impurity concentrations experimentally allowed, which suggests that the phenomenon is due to a single magnetic impurity. Kondo suggested the simplest model considering the local exchange interaction J between the magnetic impurity and itinerant electrons at the impurity site from these observations [23],

$$H_K = H_0 + J(\mathbf{s}\cdot\mathbf{S})\,. \tag{1.3}$$

Here $H_0 = \sum_{ks} \xi_k \psi^\dagger_{ks}\psi_{ks}$ describes the noninteracting electron gas (ξ_k are single-particle energies of itinerant electrons), $\mathbf{s} = \frac{1}{2}\sum_{kk'ss'} \psi^\dagger_{ks}\hat{\boldsymbol{\sigma}}_{ss'}\psi_{k's'}$ is the spin density of itinerant electrons at the impurity site (with the Pauli spin matrices $\hat{\boldsymbol{\sigma}} = (\hat{\sigma}^x, \hat{\sigma}^y, \hat{\sigma}^z)$), and $\mathbf{S}$ is the spin-1/2 operator for the magnetic impurity.

It should be noted that the phenomenological Kondo model Eq. (1.3) (in other words, the *s*-*d* model) can be reduced from the microscopic Anderson impurity model

with the help of the Schrieffer-Wolff transformation [26, 27]

$$H = H_0 + E_d \sum_\sigma n_{d\sigma} + U n_{d\uparrow} n_{d\downarrow} + \sum_{k\sigma} V_{kd} c^\dagger_{k\sigma} c_{k\sigma} + \text{H.c.}, \tag{1.4}$$

where

$$\begin{aligned} H_0 &= \sum_{k\sigma} \epsilon_k n_{k\sigma} \\ \Delta(\omega) &= \sum_k |V_{kd}|^2 \delta(\omega - \epsilon_k) \end{aligned}$$

and the Coulomb interaction

$$U = \int \phi^*_d(r) \phi^*_d(r') \frac{e^2}{|\mathbf{r} - \mathbf{r}'|} \phi_d(r) \phi_d(r') d\mathbf{r} d\mathbf{r}'$$

(here, the Bloch wavefunction ϕ).

According to Kondo [23], the lowest order of perturbation theory in the exchange constant J is not sufficient to show the logarithmic dependence in Eq. (1.2) due to the non-commutativity of the spin operators in the model, Eq. (1.3). Beyond the Born approximation, however, Kondo showed that the logarithmic temperature dependence appears in the third order in J [23],

$$\delta\rho \sim n_i \, (\nu J)^2 \big[1 + 2\nu J \ln(D_0/T)\big]. \tag{1.5}$$

Here, ν is the density of states of itinerant electrons (as a result, $\nu J \ll 1$ is a dimensionless parameter) and $D_0 \sim \epsilon_F$ is the high-energy cutoff in Eq. (1.3).

Further study after Kondo showed that logarithmically-divergent terms exist in all orders of perturbation theory, eventually leading to a geometric series [28]

$$\delta\rho(T)/\delta\rho(0) \propto \left\{ \sum_{n=0}^{\infty} (\nu J)^n \big[\ln(D_0/T)\big]^{n-1} \right\}^2 = \left[\frac{\nu J}{1 - \nu J \ln(D_0/T)} \right]^2. \tag{1.6}$$

Rewriting this sum, bearing Eq. (1.1) in mind, reads

$$\delta\rho(T)/\delta\rho(0) \propto \big[\ln(T/T_K)\big]^{-2}, \tag{1.7}$$

with the Kondo temperature T_K (characteristic energy scale in Eq. (1.1)) defined by

$$\ln(D_0/T_K) = (\nu J)^{-1}. \tag{1.8}$$

Eq. (1.8) gives the estimate of T_K with logarithmic accuracy. A more accurate estimate from Renormalization Group, see Appendix A, reads

$$T_K \simeq D_0(\nu J)^{1/2} \exp(-1/\nu J). \tag{1.9}$$

It should be noted that the Kondo effect does not always bring out the increase of the resistance like Eq. (1.7) when lowering the temperature. In fact, the Kondo effect increases the probability for an electron to scatter off the impurity by forming a resonant ground state. Thus, the scattering probability increases when the energy of the scattered electron is close to the Fermi level due to the resonance. For a magnetic impurity in a bulk sample, the scattering probability off the impurity contributes to the resistivity increase as a result of non-specific orientation of scattered electrons, as in the conventional Kondo effect.

On the other hand, for a impurity in a tunneling barrier splitting two conductors, the increased scattering probability turns into the probability for an electron to tunnel through the barrier, and the differential conductance thus increases when decreasing the external parameters in Eq. (1.1). These zero-bias anomalies in differential conductance are also the signature of the Kondo effect, and are well understood in this context [29, 30, 31].

1.1.1 Renormalization Group

Eq. (1.7) is the leading term of the asymptotic expansion of the resistivity in powers of $1/\ln(T/T_K)$, and represents the impurity contribution to the resistivity in the leading logarithmic approximation. As explained above, it is a result of summing up the most diverging terms in all orders of perturbation theory. Moreover, it turns out that the Kondo temperature, Eq. (1.8) is a non-analytic function of J. One

needs to come up with a better approach to resolve these issues. For a prescription, the Renormalization Group (RG), which is to be used in later chapters, provides the mathematical framework to study the Kondo effect in this thesis. RG [32] is based on the fact that the main contribution to observable quantities are from the electronic spectrum proportional to the temperature $\sim T$ about the Fermi level. At temperatures of the order of T_K, when the Kondo effect governs the low temperature physics, the spectrum of relevance becomes much narrower ($\sim T_K$) compared to the bandwidth D_0 of the Hamiltonian (1.3).

The exchange interaction in Eq. (1.3) induces transitions between the states near the Fermi level and the states near the band edges. Any such transition costs high energy ($\sim D_0$), and, therefore, can only occur virtually. Virtual transitions via the states near the band edges result in the second-order correction $\sim J^2/D_0$ to the exchange amplitude J for states in the proximity to the Fermi level. Consider a narrow strip of energies $\delta D \ll D_0$ near the band edge. As the strip contains $\nu\delta D$ electronic states, the total correction to the exchange amplitude due to virtual transitions is [32]

$$\delta J \sim \nu J^2 \delta D/D_0.$$

This correction is hence reflected on the exchange constant in the effective Hamiltonian $\widetilde{H}$, which has the same form as the original Kondo hamiltonian (1.3), except that it is defined for reduced energy bandwidth $D_0 - \delta D$, $|\xi_k| < D_0 - \delta D$. The renormalized exchange constant reads

$$J_{D_0-\delta D} = J_{D_0} + \nu J_{D_0}^2 \frac{\delta D}{D_0}\,, \tag{1.10}$$

with J_{D_0} in the original Hamiltonian.

Reducing the bandwidth by infinitesimal δD can be considered as a continuous process during which the original Hamiltonian (1.3) with $D = D_0$ is transformed to the effective Hamiltonian with the bandwidth $D \ll D_0$. From Eq. (1.10), one then

gets the differential scaling equation of the exchange constant [32, 33]

$$\frac{dJ_D}{d\zeta} = \nu J_D^2, \quad \zeta = \ln\left(D_0/D\right). \tag{1.11}$$

This form of the scaling equation above is quite common in the Kondo effect up to the second order in J. The solution of the scaling equation with the initial condition $J_{D_0} = J$ is

$$\nu J_D = \frac{1}{\ln(D/T_K)} \tag{1.12}$$

with the scaling invariant $T_K = D_0 \exp(-1/\nu J)$ (the Kondo temperature). The reduction of the bandwidth in RG can be treated as a unitary transformation that decouples the high energy states near the band edges from the rest [34, 35, 36, 37] (this point of view is discussed in the Appendix A). Any such transformation should also affect the operators of the observable quantities. However, the "current" operator is not affected during RG, and evaluation of the conductivity (and resistivity) can be carried out at any stage of RG, yielding the same result.

The whole advantage of RG becomes apparent when it is pushed to its limit. The renormalization Eq. (1.11) works until the bandwidth D becomes of the order of the energy scale $\sim T$ of real transitions. At this termination of RG, the third-order correction to the resistivity in Eq. (1.5) is ignorable, whereas the main (second-order) contribution takes the form

$$\delta\rho(T)/\delta\rho(0) \propto \left(\nu J_{D\sim T}\right)^2 = \left[\ln(T/T_K)\right]^{-2}, \tag{1.13}$$

consistent with Eq. (1.7) of perturbation theory.

1.1.2 Kondo singlet

We next replace the local spin density of itinerant electrons $\mathbf{s}$ in Eq. (1.3) with a single spin-1/2 operator $\mathbf{S}'$ to capture the idea of the Kondo effect and the Kondo singlet in many body systems. The ground state of this toy model of two spins $H' = J(\mathbf{S}' \cdot \mathbf{S})$ is a spin singlet for the antiferromagnetic case $J > 0$ (a triplet for the ferromagnetic

one $J < 0$). The excitation energy for a triplet is J. This energy J can be viewed as the binding energy of the singlet.

Turning back to the Kondo Hamiltonian, one would expect the analogy of this spin singlet in the Kondo model. However, $\mathbf{s}$ (instead of a single spin $\mathbf{S}'$) in Eq. (1.3) is a spin density of itinerant electrons at the impurity site. It is therefore difficult for the impurity to capture an itinerant electron and form a singlet as in the toy model. Nevertheless, RG suggests that even a weak bare exchange constant becomes effectively strong for the electrons close to the Fermi level, see Eq. (1.11), and therefore suffices to form a singlet ground state [32, 38, 39, 40] – the Kondo singlet. The binding energy for this Kondo singlet is not the exchange constant J but the exponentially small Kondo temperature T_K in Eq. (1.8).

It should be noted that the Kondo effect lifts the degeneracy of the ground state. It is the main reason for the logarithmic divergences in perturbation theory, too. By taking $J = 0$ as usual in perturbation theory, the ground state is doubly degenerate as a spin-up and spin-down state of the impurity. Then, perturbation theory in J is applicable when the temperature is greater than the binding energy for the Kondo singlet, *i.e.*, $T \gg T_K$, and the result is Eq. (1.7)

$$\delta\rho(T)/\delta\rho(0) \propto \left[\ln(T/T_K)\right]^{-2}.$$

In the opposite limit $T \ll T_K$, Fermi liquid theory (beyond the scope of this thesis) reads [41],

$$1 - \delta\rho(T)/\delta\rho(0) \propto (T/T_K)^2, \quad T \ll T_K. \tag{1.14}$$

To summarize, Eqs. (1.7) and (1.14) are valid in the weak ($T \gg T_K$) and strong ($T \ll T_K$) coupling limits, respectively. In addition, the Kondo effect is a crossover phenomenon, unlike a phase transition [32, 38, 39, 40], and thus the resistivity $\delta\rho(T)/\delta\rho(0)$ is a smooth function in the crossover region of $T \sim T_K$.

1.2 Coulomb blockade in a quantum dot

In recent years, interest in the Kondo effect grew again [42] due to advances in experimental techniques as well as nanoscale fabrication. Progress in fabrication enables one to design artificial nanoscale magnetic impurities. Contemporary experimental techniques provide direct access to transport properties of such artificial impurities as well.

The Coulomb blockade [20, 21, 43, 44, 45, 46] is the key to understanding the nanoscale phenomena, especially quantum transport. The Coulomb blockade were first reported in several pioneering experiments [47, 48, 49, 50, 51]. In a single electron transistor (SET) setup [43, 44, 45], a quantum dot is connected to two conducting leads L and R via tunneling junctions and is capacitively coupled to the gate in Fig. 1.1.

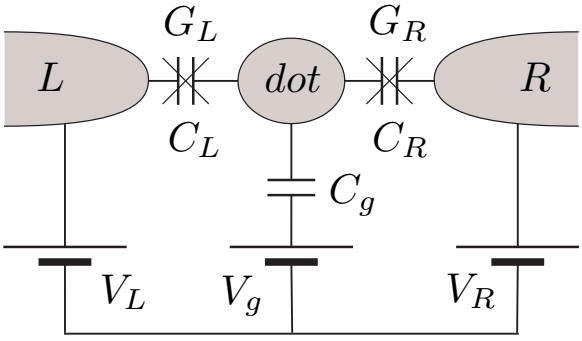

Figure 1.1: Equivalent circuit for a quantum dot connected to two massive conducting leads by tunnel junctions with conductances $G_{L,R}$ and capacitances $C_{L,R}$ and capacitively coupled to the gate electrode V_g, adopted from Pustilnik and reprinted with the permission of John Wiley and Sons.

The electrostatic energy of a dot with charge Q is classically

$$E(Q) = \frac{Q^2}{2C} - Q\frac{C_g}{C}V_g, \tag{1.15}$$

where $C = C_L + C_R + C_g$ is the total capacitance of the dot, and V_g is the potential on the gate, see Fig. 1.1. Plugging $Q = eN$ into the energy, where N is the number

of excess electrons in the dot, one obtains

$$E(N) = E_C\big(N - N_0\big)^2 + \text{const}, \tag{1.16}$$

where $E_C = e^2/2C$ is the charging energy and $N_0 = C_g V_g/e$ is the dimensionless gate voltage.

1.2.1 Model of a lateral quantum dot system

The simplest Hamiltonian for the dot accounting for the electrostatic energy (1.16) is

$$H_d = \sum_{ns} \epsilon_n d^\dagger_{ns} d_{ns} + E_C\big(\hat{N} - N_0\big)^2. \tag{1.17}$$

Here, the first term represents the single-particle (noninteracting) part, and the second term is from Eq. (1.16) after replacing N with the corresponding number operator $\hat{N} = \sum_{ns} d^\dagger_{ns} d_{ns}$.

The Hamiltonian (1.17) (known as the Constant Interaction Model) could be justified microscopically [20, 21, 46] for dots with no spatial symmetries, which are large compared with the effective Bohr radius $a_0 = \kappa\hbar^2/e^2 m$ (here m is the effective mass, and κ is the dielectric constant). Both conditions are usually satisfied for lateral quantum dots formed by the electrostatic depletion of the two-dimensional electron gas at the interface of semiconductor heterostructure such as GaAs/AlGaAs [4, 43, 44, 45]. For a ballistic 2D dot of linear size L, the capacitance $C \sim \kappa L$ and the mean level spacing between the single-particle energy levels can be estimated as $\delta \sim \hbar^2/mL^2$. Accordingly,

$$E_C/\delta \sim L/a_0 \gg 1. \tag{1.18}$$

For example, for GaAs-based semiconductor quantum dot systems [1, 2, 4, 5, 6, 7, 8, 9, 10, 43, 44, 45], $a_0 \approx 10$ nm, and a relatively small dot with $L \sim 100$ nm contains about 10 electrons. The charging energy of such a dot is of the order $E_C \sim 1$ meV, while the mean single-particle level spacing δ is roughly 10 times smaller. Hence, both the charging effects and the effects associated with the quantization of the

single-particle energy levels can be resolved in transport experiments performed in dilution refrigerators with base temperatures below 50 mK [43, 44, 45].

The electrostatic potential defining lateral quantum dot systems varies smoothly on the scale of the de Broglie wavelength at the Fermi energy. Dot-lead junctions thus act as electronic waveguides with a well-defined number of propagating modes of an electronic wave. The Coulomb blockade emerges when the last propagating mode in each junctions is pinched off. This allows one to model the leads as reservoirs of one-dimensional electrons [20, 21, 46, 52, 53],

$$H_{\text{leads}} = \sum_{\alpha k s} \xi_k c^\dagger_{\alpha k s} c_{\alpha k s}, \quad \alpha = R, L \tag{1.19}$$

with the density of states ν. Tunneling between the dot and the leads is

$$H_{\text{tunneling}} = \sum_{\alpha k n s} t_\alpha c^\dagger_{\alpha k s} d_{n s} + \text{H.c.}, \tag{1.20}$$

where we neglected the dependence of the tunneling amplitudes on n (see the discussion in Chapter 2 and Appendix B) without loss of generality, so that each single-particle energy level in the dot acquires the same level-width $\Gamma_\alpha = \pi t_\alpha^2$ due to the tunneling to lead α.

The conductance G_α of the dot-lead junction due to tunneling is

$$G_\alpha = (4e^2/\hbar)(\Gamma_\alpha/\delta).$$

The tunneling Hamiltonian Eq. (1.20) is valid for an almost closed dot, *i.e.*, when $G_\alpha \ll e^2/h$, and hence the total width $\Gamma_0 = \Gamma_L + \Gamma_R$, the mean level spacing δ, and the charging energy E_C establish a well-defined hierarchy in a later quantum dot

$$\Gamma_0 \ll \delta \ll E_C. \tag{1.21}$$

1.2.2 Charge quantization and Coulomb blockade oscillations

Let's consider an isolated dot ($t_\alpha \to 0$) where the number of electrons N in the dot is a good quantum number at low temperatures. The electrostatic energy to add an

electron to the dot is

$$E_{N+1} - E_N = 2E_C\big(N_0^* - N_0\big), \quad N_0^* = N + 1/2 = \text{half-integer}.$$

From this, one sees that the N and $N+1$ electron states are degenerate at each $N_0 = N_0^* =$ half-integer. At low enough temperatures $T \ll E_C$, the average number of electrons $N(N_0) = \langle \hat{N} \rangle$ over the dimensionless gate N_0 should be staircase-like as in Fig. 1.2(a) with the step-width $\Delta \sim T/E_C$. These regions in the vicinity of the degeneracy within Δ are called the mixed-valence regions. In other words, the charge quantization is expected over the entire region of the gate voltage except for the mixed-valence regions. The charge quantization remains intact at low temperatures, even when the tunneling is introduced. At very low temperatures $T \lesssim \Gamma$, however, the step-width $\Delta \sim \Gamma/E_c$ comes with the renormalized level-width $\Gamma \gtrsim \Gamma_0$ (see Chapter 2) instead of the temperature T, and hence the width of the mixed-valence regions is renormalized as well.

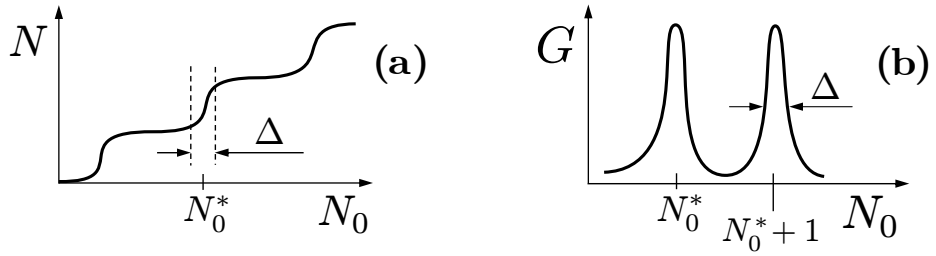

Figure 1.2: (a) Average number of electrons in a dot $N = \langle \hat{N} \rangle$ at $T \ll E_C$ as a function of the dimensionless gate voltage N_0. The number of electrons N differs significantly from integer values in the narrow mixed-valence regions of the width $\Delta \sim \max\{\Gamma, T\}/E_C$ about $N_0 = N_0^* =$ half-integer.
(b) At $\Gamma \lesssim T \ll E_C$ the conductance is small in the wide Coulomb valley of the width of almost 1 in the dimensionless gate voltage due to the Coulomb blockade.
Adopted from Pustilnik and reprinted with the permission of John Wiley and Sons.

The charge quantization in the dot translates into the conductance G through the dot. At high temperature $T \gg E_C$, the Coulomb interaction in Eq. (1.17) (and hence the gate voltage dependence) has no effect since the thermal excitation is big enough to wipe out the staircase-like charge quantization. The conductance in this high-T

limit is small, $G_\infty \ll e^2/h$, and the classical resistance addition formula gives

$$\frac{1}{G_\infty} = \frac{1}{G_L} + \frac{1}{G_R}\,. \tag{1.22}$$

Things change dramatically at low temperatures. The conductance starts to depend on the gate voltage N_0 at all $T \lesssim E_C$. When the gate voltage is outside the mixed-valence regions, in Fig. 1.2(a), adding or removing an electron costs approximately the charging energy E_C in Eq. (1.17). From the energy conservation for a real transition, the probability to have an electron with energy E_C is proportional to $\exp(-E_C/T)$ outside the mixed-valence regions. That is, the conductance is exponentially suppressed at $T \ll E_c$ (Coulomb blockade valley, hereafter CB valley). On the other hand, the energy cost in the mixed-valence regions is much smaller due to the degeneracy, and the conductance is relatively large in these regions (Coulomb blockade peak, hereafter CB peak)

In the low-T limit, *i.e.*, at $T \ll E_C$, the conductance $G(N_0)$ displays a quasi-periodic behavior of narrow CB peaks of the width $\Delta \ll 1$ accompanied by wide CB valleys in Fig. 1.2(b). In terms of the dimensionless gate voltage N_0, the spacing between two neighboring CB peaks ≈ 1 in Fig. 1.2(b).

Thorough study on the Coulomb blockade was done in the light of the orthodox theory by Shekhter [54, 55, 56, 57, 58]. The orthodox theory is based on the rate equation formalism at $T \gg \delta$ (Numerical approach to solve the rate equations of a quantum dot is shown in Bonet [59]). The orthodox theory assumes that the inelastic electron relaxation rate in a dot is large compared with the electron escape rate $\Gamma/\hbar$. In this approximation, the tunneling via each junction through the dot can be treated as an independent process.

According to the orthodox theory, the Coulomb blockade peaks saturate to half of their high-temperature conductance G_∞ when decreasing T. However, the discreteness of the energy levels becomes more relevant at $T \ll \delta$. The rate equation formalism is yet applicable at $T \gg \Gamma$ [60, 61], and the Coulomb blockade peaks

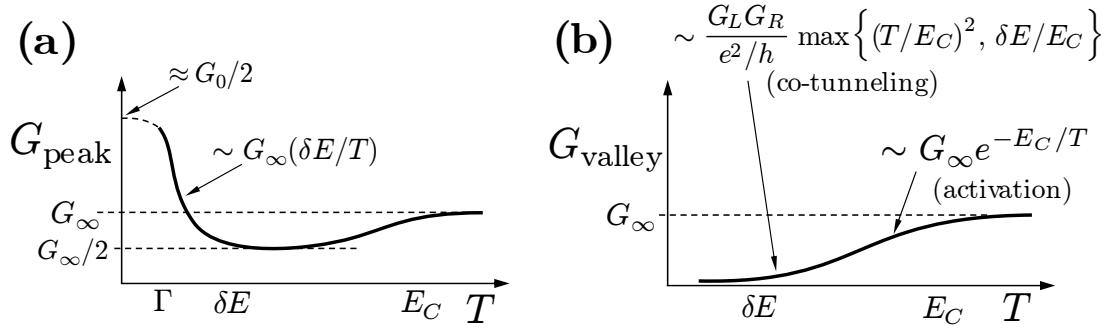

Figure 1.3: (a) The height of a Coulomb blockade peak *vs.* the temperature in the mixed-valence regions.
(b) Conductance *vs.* the temperature in the middle of a Coulomb blockade valley.
Adopted from Pustilnik and reprinted with the permission of John Wiley and Sons.

increase as in Fig. 1.3(a) up to $\sim e^2/h \gg G_\infty$ [46, 60, 61].

In the Coulomb blockade valleys, the real transitions are strongly suppressed due to the low thermal activated transport at low temperatures, as explained. But, the virtual transitions of high order process could yet contribute to the conductance in Fig. 1.3(b). In this co-tunneling mechanism in Fig. 1.4, the virtual transitions are not restricted by energy conservation. Thus, the tunneling from one lead into the dot, and tunneling from the dot to the another lead is a single quantum process, for example, from the left lead to right lead in Fig. 1.4 [47, 48, 62].

The co-tunneling contribution is very sensitive to the tunneling amplitudes in Eq. (1.20) as well as to the details of the model. In particular, the result in Fig. 1.3(b) is valid for large chaotic semiconductor quantum dots [43, 44, 45, 62], as is our case. In this case, it is well-known that the elastic co-tunneling is the main source of the mesoscopic fluctuations in the Coulomb blockade valleys at all temperatures $T \lesssim E_C$ [63, 46, 20, 21].

1.3 Kondo effect in a single electron transistor

In order for the artificial impurity to be spin like in the conventional Kondo model, N in the dot must be obviously odd-integer in the Coulomb valleys. The uppermost

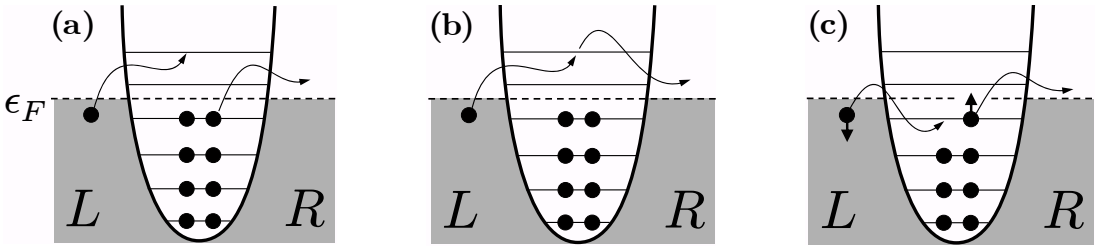

Figure 1.4: Various second-order (co-tunneling) processes adopted from Averin *et al.*
(a) Inelastic co-tunneling: an electron tunnels from the left lead into one of the unoccupied single-particle levels in the dot, whereas an electron occupying some other level tunnels out to the right lead, leaving an electron-hole pair behind. The contribution to the conductance scales with temperature as T^2.
(b) Elastic co-tunneling: unlike the in-elastic case, occupation of electrons in the dot is the same through the co-tunneling process. This contribution to the conductance is T-independent.
(c) Spin-flip co-tunneling process: the origin of the Kondo effect in the dot.
Adopted from Pustilnik ad reprinted with the permission of John Wiley and Sons.

level in the dot is singly occupied in the ground state, which is either a spin-up or a spin-down state of the electron. Now, the artificial impurity is magnetic and doubly degenerate with a spin $S = 1/2$. This singly-occupied level is a key element in transport at low temperatures $T \ll E_c$, as a source of a elastic co-tunneling spin-flip process in Fig. 1.4(c). This is the same spin-flip process of a magnetic impurity in a host metal, which is the origin of the Kondo effect in a quantum dot [29, 30, 31, 64, 65]. So, an odd number of electrons in the dot are not subject to the Coulomb blockade at $T \to 0$. Hence, one expects the enhanced conductance in the Coulomb valleys when lowering the temperature in Fig. 1.5(a) only when there are odd number of electrons.

To reduce the quantum dot Hamiltonian to the Kondo model, one has to work on the Hamiltonian Eqs. (1.19)-(1.20). Instead of the conduction electron operators $c_{R,(L)}$ in the right (left) leads, one can introduce linear combinations to decouple the irrelevant operators,

$$\begin{pmatrix} c \\ c' \end{pmatrix} = \left(t_R^2 + t_L^2\right)^{-1/2} \begin{pmatrix} t_R & t_L \\ -t_L & t_R \end{pmatrix} \begin{pmatrix} c_R \\ c_L \end{pmatrix}. \tag{1.23}$$

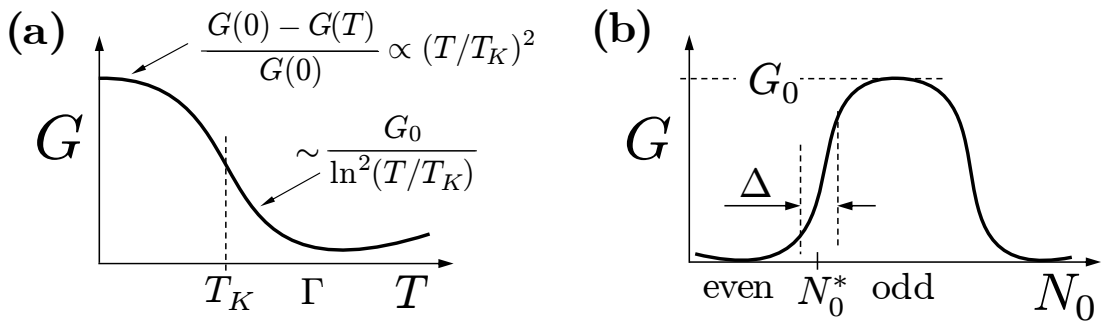

Figure 1.5: (a) The conductance *vs.* the temperature in the Coulomb blockade valley with an odd number of electrons in the dot.
(b) Conductance *vs.* the gate voltage at $T \to 0$.
Adopted from Pustilnik and reprinted with the permission of John Wiley and Sons.

Without dependence on n, it is clear from Eqs. (1.19) and (1.20) that only c-electrons in the new basis couple to the dot [66]. The effective Hamiltonian with c-electrons becomes (decoupling c'-electrons)

$$H = \sum_{ks} \xi_k c_{ks}^\dagger c_{ks} + t_0 \sum_{kns} \left(c_{ks}^\dagger d_{ns} + \text{H.c.} \right) + \sum_{ns} \epsilon_n d_{ns}^\dagger d_{ns} + E_C \left(\hat{N} - N_0 \right)^2 \qquad (1.24)$$

with the tunneling amplitude $t_0 = \sqrt{t_R^2 + t_L^2}$ in the new basis. Eq. (1.24) is the simplest multilevel generalization of the Anderson impurity model, Eq. (1.4), in the dot [26]. For $N \approx$ odd integer, it could be further reduced to the Kondo Hamiltonian Eq. (1.3).

$$H_K = H_0 + J(\mathbf{s} \cdot \mathbf{S})$$

The spin operator $\mathbf{S}$ here represents the spin doublet of the ground state of the dot equivalent to the magnetic impurity spin, and the estimation of the exchange constant reads

$$J \sim \frac{t_0^2}{\min\{E_\pm\}}, \qquad (1.25)$$

where $E_\pm$ is the electrostatic energy to add (remove) an electron to (from) the dot. It should be noted that the exchange interaction describes a second-order process in Fig. 1.4(c), which comes with two tunneling events, the factor t_0^2, and an intermediate virtual state with $N \pm 1$ electrons in the dot via a spin-flip process. The energy

cost via virtual transition is $E_\pm$, hence the factor $\min\{E_\pm\}$ in the denominator. According to Eq. (1.25), the dependence of the exchange constant (and, therefore, of the Kondo temperature) on the gate voltage N_0 is nonmonotonic, with a minimum in the middle of the Coulomb blockade valleys. At this point, $E_\pm = E_C$ and $\min\{J\} \sim t_0^2/E_C$. While the estimate (1.25) is qualitatively correct, actual dependence of the exchange constant on the gate voltage turns out to be much more complicated than that prescribed by Eq. (1.25). Understanding this dependence is the main goal of this thesis, and is described in details in the Chap. 2.

First, we briefly describe the conductance at zero temperature due to the Kondo effect. Since the Kondo effect lifts the degeneracy at any gate voltage, one could use the Landauer formula to calculate the conductance via the transmission probability through the dot. According to the scattering theory [67], the transmission probability is related to the scattering phase shifts of the itinerant electrons. As shown earlier, only c-electrons are coupled to the dot and scattered off in the model. The conductance is given by [20, 21]

$$G = G_0 \frac{1}{2} \sum_s \sin^2 \delta_s, \tag{1.26}$$

where δ_s is the phase shift at the Fermi level of c-electrons with spin s, and

$$G_0 = \frac{2e^2}{h} \left[\frac{2t_L t_R}{t_L^2 + t_R^2} \right]^2. \tag{1.27}$$

Fortunately, the Friedel sum rule relates the occupation number to the phase shifts in the model

$$\delta_s = \pi N_s, \quad N_s = \Big\langle \sum_n d_{ns}^\dagger d_{ns} \Big\rangle.$$

The Kondo singlet reads $N_s = N/2$ for both spin states, Eq. (1.26) then gives

$$G = G_0 \sin^2(\pi N/2). \tag{1.28}$$

From this, one can see the conductance reaches its maximum G_0 at $N =$ odd integer in the Coulomb valleys in Fig. 1.5(b) at zero temperature, which is the signature of the Kondo effect.

CHAPTER II

KONDO TEMPERATURE OF A QUANTUM DOT.

As discussed in Chapter 1, at certain gate voltages, the conductance of a quantum dot system increases with the decrease of temperature. The increase takes place when the dot has an odd number of electrons, and, therefore, has a non-zero spin in the ground state. Moreover, the dependence of the conductance on temperature is logarithmic. These facts suggest that the origin of the enhanced conductance is the Kondo effect, with the dot behaving essentially as an artificial magnetic impurity.

As mentioned above, for odd N a generic model of a quantum dot system is equivalent at low energies to an appropriate Kondo model (1.3). In this chapter, we demonstrate this equivalence explicitly, and discuss the dependence of the exchange amplitude (hence, the Kondo temperature) on the gate voltage N_0.

Our starting point is the Constant Interaction Model

$$H = \sum_{ks} \xi_k c_{ks}^\dagger c_{ks} + \sum_{ns} \epsilon_n d_{ns}^\dagger d_{ns} + E_C\big(\hat{N} - N_0\big)^2 + t_0 \sum_{kns} \big(c_{ks}^\dagger d_{ns} + \text{H.c.}\big), \qquad (2.1)$$

introduced in Eq. (1.24) above. Without loss of generality, we assume that the Fermi level in the dot corresponds to $\epsilon_0 = 0$. Otherwise, the single-particle levels in the dot ϵ_n are characterized by a finite level spacing δ. For lateral quantum dot systems in the weak tunneling regime, the tunneling-induced level width $\Gamma_0 = \pi\nu t_0^2$, the level spacing δ, and the charging energy E_C form a well-defined hierarchy $\Gamma_0 \ll \delta \ll E_C$, see Eq. (1.21).

For N_0 tuned away from the mixed valence regions, at

$$N_0 \approx N^* = \text{odd integer}$$

(notice the difference between integer N^* and half-integer N_0^* introduced in Chapter 2)

the dot has an odd number of electrons $N = \langle \hat{N} \rangle \approx N^*$, and its ground state has spin $S = 1/2$. In the low-energy sector, both charge excitations of the dot, characterized by the energy cost to add/remove an electron

$$E_\pm = 2E_C \big| N_0 - N^* \mp 1/2 \big|, \tag{2.2}$$

and the intradot excitations (the corresponding cost is the level spacing δ) are absent. Our strategy is to project Eq. (2.1) onto this low-energy domain, and the projection will result in the effective Hamiltonian with the bandwidth

$$D_0 = \min\{\delta, E_\pm\}. \tag{2.3}$$

As the first step, we project Eq. (2.1) onto the three lowest-energy charge states of the dot, $|N\rangle$ and $|N \pm 1\rangle$, which gives

$$H = H_c + H_t^+ + H_t^- + H_d, \tag{2.4}$$

where $H_c = \sum_{ks} \xi_k c_{ks}^\dagger c_{ks}$ describes the conduction electrons,

$$H_t^+ = t_0 \sum_{kns} c_{ks}^\dagger d_{ns} \, |N+1\rangle\langle N| + \text{H.c.}, \tag{2.5}$$

$$H_t^- = t_0 \sum_{kns} c_{ks}^\dagger d_{ns} \, |N\rangle\langle N-1| + \text{H.c.}, \tag{2.6}$$

describe the tunneling, and

$$H_d = \sum_{ns} \epsilon_n d_{ns}^\dagger d_{ns} + E_+ \, |N+1\rangle\langle N+1| + E_- \, |N-1\rangle\langle N-1| \, . \tag{2.7}$$

describes the isolated dot.

The next step depends on the relation between δ and E_C. We discuss first the (unphysical) limit $\delta \gg E_C$, corresponding to the single-level Anderson impurity model [26, 68, 69].

2.1 Anderson model: $\delta \gg E_C$

For $\delta \gg E_C$ all but $n = 0$ energy levels in the dot are either empty or doubly occupied. Projecting these levels out, we write $H_d \to 2E_C \left[n_\uparrow n_\downarrow - (N_0 - 1/2)(n_\uparrow + n_\downarrow) \right]$, where

$n_\uparrow$ and $n_\downarrow$ are spin-up and spin-down occupations of the $n = 0$ level. At energies lower than $E_\pm$, tunneling-induced transitions to states with $N \pm 1$ electrons in the dot are virtual. To second order in tunneling amplitude, these transitions can be taken into account by means of the Schrieffer-Wolff transformation [27].

Consider a unitary transformation

$$H \to e^S H e^{-S}, \quad S = -S^\dagger$$

with $S \propto t_0$. Applying the Baker-Hausdorff formula, we find

$$e^S H e^{-S} = H_c + H_d + \underbrace{H_t + \big[S, H_c + H_d\big]}_{\propto t_0} + \underbrace{\big[S, H_t\big] + \frac{1}{2}\big[S, [S, H_c + H_d]\big]}_{\propto t_0^2} + O(t_0^3)$$

If S satisfies

$$H_t + \big[S, H_c + H_d\big] = 0, \tag{2.8}$$

the first-order contribution is absent, and

$$e^S H e^{-S} \approx H_c + H_d + \frac{1}{2}\big[S, H_t\big]. \tag{2.9}$$

The generator of the transformation, satisfying Eq. (2.8), is given by

$$S = S_+ + S_-$$

with

$$S_+ = \sum_{ks} \frac{t_0}{\xi_k + E_+} c_{ks}^\dagger d_{0s} \, |N+1\rangle\langle N| - \text{H.c.}, \tag{2.10}$$
$$S_- = \sum_{ks} \frac{t_0}{\xi_k + E_-} d_{0s}^\dagger c_{ks} \, |N-1\rangle\langle N| - \text{H.c.}$$

Using Eqs. (2.9) and (2.10), the identity

$$2\,\delta_{s_1 s_2}\delta_{s_1' s_2'} = \delta_{s_1 s_1'}\delta_{s_2' s_2} + \boldsymbol{\sigma}_{s_1 s_1'} \cdot \boldsymbol{\sigma}_{s_2' s_2}, \tag{2.11}$$

(here $\boldsymbol{\sigma} = (\sigma^x, \sigma^y, \sigma^z)$ are the Pauli matrices), and projecting the result onto the subspace of the Hilbert space with N electrons on the dot, we arrive at the Kondo Hamiltonian

$$H = H_c + V\rho + J(\mathbf{s} \cdot \mathbf{S}), \tag{2.12}$$

where $\rho = \sum_{kk's} c^\dagger_{ks} c_{k's}$ and $\mathbf{s} = \sum_{kk'ss'} c^\dagger_{ks} (\boldsymbol{\sigma}_{ss'}/2) c_{k's'}$ represent the local particle and spin density of conduction electrons, and the spin $\mathbf{S}$ describes the state of the dot.

The amplitude of the potential scattering in Eq. (2.12) reads

$$V = -\frac{t_0^2}{2}\left(\frac{1}{E_+} - \frac{1}{E_-}\right). \tag{2.13}$$

This term breaks the particle-hole symmetry of the model, thus reflecting the deviation of the number of electrons in the dot N from the integer value N^* [70],

$$\Delta N = N - N^* \approx -2\nu V. \tag{2.14}$$

When the gate voltage approaches the mixed-valence region, say, at $N_0 \approx N^* + 1/2$, Eq. (2.14) reduces to $V \approx -t_0^2/2E_+$. The requirement of N being close to an integer $|\Delta N| \ll 1$ and Eqs. (2.2) and (2.14) then give

$$\left|N_0 - N^* \pm 1/2\right| \gg \Gamma_0/E_C, \tag{2.15}$$

which implies that the mixed-valence regions in the Anderson model have width $\sim \Gamma_0/E_C$, in agreement with [68, 69].

The exchange amplitude in Eq. (2.12) is given by

$$J = 2t_0^2\left(\frac{1}{E_+} + \frac{1}{E_-}\right) = \frac{J_0}{1 - 4(N_0 - N^*)^2} \tag{2.16}$$

with

$$\nu J_0 = \frac{4\nu t_0^2}{E_C} = \frac{4}{\pi}\frac{\Gamma_0}{E_C}. \tag{2.17}$$

The exchange amplitude (2.16) (and, therefore, T_K) has a minimum at the particle-hole symmetric point $N_0 = N^*$, where $J\big|_{N_0=N^*} = J_0$. Accounting for higher orders in t_0 contributions (which amounts to going beyond the accuracy of the Schrieffer-Wolff transformation) merely results in a small correction [68, 69, 71],

$$\Delta J_0/J_0 \sim \nu J_0 \ll 1. \tag{2.18}$$

The Anderson model therefore provides a qualitatively correct description of the dependence $T_K(N_0)$. The dependence is non-monotonic with a minimum in the middle of the Coulomb blockade valley. This is why Eq. (1.9) with D_0 and J given by Eqs. (2.3) and (2.16) is often employed to fit the experimental data, see, e.g., [4, 5, 6].

2.2 Realistic quantum dot: $\delta \ll E_C$

We turn now to the realistic limit $\delta \ll E_C$. Although the Anderson model is no longer applicable in this limit, its prediction for $\min\{J(N_0)\} = J_0$, see Eqs. (2.16) and (2.17), remain intact. Instead of Eq. (2.18), the leading correction now reads [71]

$$\Delta J_0/J_0 \sim \frac{\Gamma_0}{\delta}\left[1+\alpha\,\frac{\ln(E_C/\delta)}{E_C/\delta}\right], \tag{2.19}$$

where $\alpha \sim 1$ is a numerical coefficient [71]. Although the correction (2.19) is larger than that in the Anderson model by a factor $E_C/\delta \gg 1$, see Eq. (2.18), the separation of the energy scales Eq. (1.21) ensures that it is still relatively small, $\Delta J_0/J_0 \ll 1$.

This changes dramatically [72] when the gate voltage is tuned away form the middle of the Coulomb blockade valley $N_0 = N^*$. Indeed, it is well-known [73] that when the gate voltage is close to (but still outside) the mixed valence region, say, at

$$\Gamma_0/E_C \ll N^* - N_0 + 1/2 \ll 1 \tag{2.20}$$

(more careful estimate is given below), transitions between the two almost degenerate charge states of the dot $|N\rangle$ and $|N+1\rangle$ result in diverging logarithmic corrections to the tunneling amplitude. The origin of these corrections is again the Kondo effect, with the two charge states playing the part of the impurity spin [52, 73].

2.2.1 Kondo effect in the charge sector

To make the connection with the Kondo problem explicit, we, following [73], project out virtual transitions to the state $|N-1\rangle$, associated with high energy cost

$$E_- \approx E_C \gg E_+.$$

This amounts to the introduction of a high-energy cutoff in Eq. (2.4):

$$|\xi_k|, |\epsilon_n| < D \sim E_C.$$

The projected Hamiltonian can be brought into the form of an anisotropic two-channel Kondo model in a magnetic field with the physical spin s representing the channel index [73],

$$\begin{aligned} H &= \sum_s H_s + E_+ \hat{T}_z \\ H_s &= \sum_{p\alpha} \varepsilon_{p\alpha} \psi^\dagger_{sp\alpha} \psi_{sp\alpha} + t_z \tau^z_s \hat{T}_z + t_\perp \left(\tau^+_s \hat{T}_- + \tau^-_s \hat{T}_+ \right). \end{aligned} \tag{2.21}$$

In terms of $|\Downarrow\rangle$ and $|\Uparrow\rangle$, representing, respectively, charge states with N^* and N^*+1 electrons in the dot, the pseudospin operators in Eq. (2.21) are given by

$$\hat{T}_z = \frac{1}{2}\big(|\Uparrow\rangle\langle\Uparrow| - |\Downarrow\rangle\langle\Downarrow|\big), \quad \hat{T}_+ = \hat{T}^\dagger_- = |\Uparrow\rangle\langle\Downarrow| \,.$$

The operators ψ in (2.21) are the relabeled operators c and d of Eq. (2.1),

$$\psi_{s,p,\alpha=\Uparrow} = d_{n\to p,s} \,, \quad \psi_{s,p,\alpha=\Downarrow} = c_{k\to p,s} \,.$$

Accordingly, the single-particle energies $\varepsilon_{p,\alpha} = -\varepsilon_{-p,\alpha}$ are characterized by the pseudospin-dependent densities of states

$$\nu_\Uparrow = 1/\delta, \quad \nu_\Downarrow = \nu.$$

Finally, the local pseudospin density in Eq. (2.21) are given by

$$\boldsymbol{\tau}_s = \sum_{pp'\alpha\alpha'} \psi^\dagger_{sp\alpha} \frac{\widetilde{\boldsymbol{\sigma}}_{\alpha\alpha'}}{2} \psi_{sp'\alpha'},$$

where components of the vector $\widetilde{\boldsymbol{\sigma}}$ are the Pauli matrices acting on the pseudospin degree of freedom.

The bare (corresponding to the bandwidth $D \sim E_C$) values of the coupling constants in (2.21) are

$$t_\perp = t_0, \quad t_z = 0. \tag{2.22}$$

The derivation of the scaling equations for the model (2.21) follows closely that in Appendix A. In terms of the dimensionless coupling constants

$$I_z = \frac{1}{2}(\nu_{\Uparrow} + \nu_{\Downarrow})t_z, \quad I_\perp = 2(\nu_{\Uparrow}\nu_{\Downarrow})^{1/2}t_\perp, \tag{2.23}$$

and the running variable $\zeta = \ln(E_C/D)$, the RG equations are identical to Eqs. (A.21)-(A.23) with $M = 2$,

$$\frac{dI_z}{d\zeta} = = I_\perp^2 - I_\perp^2 I_z, \tag{2.24}$$

$$\frac{dI_\perp}{d\zeta} = I_z I_\perp - \frac{1}{2}\left(I_z^2 + I_\perp^2\right) I_\perp. \tag{2.25}$$

Renormalization also generates terms of the type $\sum_{pp'\alpha} \psi^\dagger_{sp\alpha}\psi_{sp'\alpha}\hat{T}_z$. These terms lead to small pseudospin-dependent corrections to the density of states [74], which we neglect.

Detailed analysis of the scaling equations (2.24)-(2.25) subject to the initial conditions

$$I_\perp^2(0) = 4\nu t_0^2/\delta = 4\Gamma_0/\pi\delta, \quad I_z(0) = 0, \tag{2.26}$$

see Eqs. (2.22) and (2.23), is presented in the Appendix, see Section A.1.2. The coupling constants $I_z(\zeta)$ and $I_\perp(\zeta)$ diverge at $\zeta \to \zeta_C = \ln(E_C/T_C)$, where the Kondo temperature for the charge Kondo effect is given by

$$T_C \simeq E_C\gamma_0 \exp[-\pi/2\gamma_0], \quad \gamma_0 = I_\perp(0) = \sqrt{4\Gamma_0/\pi\delta}. \tag{2.27}$$

In the so-called scaling limit (corresponding to $T_C \ll D \ll E_C$), the solutions of Eqs. (2.24)-(2.25) take the form

$$I_\perp^2(D) \approx \gamma_0^2 + I_z(D) \approx \gamma_0^2 + \frac{1}{\left[\ln(D/T_C)\right]^2}, \tag{2.28}$$

see Section A.1.2. The right hand side (hereafter, r.h.s) of Eq. (2.28) contains a sum of two contributions, the bare value of $I_\perp$, and the correction due to a logarithmic renormalization associated with the charge Kondo effect. Note that in order to obtain this result, it is crucial to take into account the third-order terms in the r.h.s. of Eqs. (2.24) and (2.25).

2.2.2 Reduction to the Kondo model

The scaling described by Eqs. (2.24)-(2.25) continues as long as the two charge states, $|N\rangle$ and $|N+1\rangle$, can be treated as degenerate, and as long as the discreteness of the dot's spectrum can be neglected. In other words, as long as the bandwidth D in Eq. (2.21) exceeds both the addition energy E_+ and the single-particle level spacing in the dot δ. At smaller D,

$$D \lesssim D^* = \max\{\delta, E_+\}, \tag{2.29}$$

the effective Hamiltonian is given by Eq. (2.21) with renormalized coupling constants. Restoring the notations of Eqs. (2.4)-(2.7), we write it as

$$\begin{aligned} H &= \sum_{ks} \xi_k c_{ks}^\dagger c_{ks} + \sum_{ns} \epsilon_n d_{ns}^\dagger d_{ns} + E_+ \left|N+1\right\rangle\!\left\langle N+1\right| \\ &\quad + t \sum_{kns} \left(c_{ks}^\dagger d_{ns} \left|N+1\right\rangle\!\left\langle N\right| + \text{H.c.}\right) \end{aligned} \tag{2.30}$$

with the renormalized tunneling amplitude given by

$$t^2 = t_\perp^2(D^*) = t_0^2 + \frac{\delta}{4\nu\left[\ln(D^*/T_C)\right]^2}\,. \tag{2.31}$$

In writing Eq. (2.30), we have omitted the potential scattering terms arising from the z-component of the exchange in Eq. (2.21).

Further reduction of the bandwidth from D^* down to D_0, see Eq. (2.3), can be carried out without regard to the presence of multiple energy levels in the dot (these levels have been already accounted for in the renormalization of the tunneling amplitude). In other words, Eq. (2.30) is equivalent to the Anderson model in the strongly anisotropic limit. Accordingly, virtual transitions to the state $|N+1\rangle$ can be taken into account by means of the Scrieffer-Wolff transformation, see Section 2.1. The transformation results in the Kondo Hamiltonian (2.12) with the exchange constant

$$\nu J = \frac{2\nu t^2}{E_+} = \frac{E_C}{2E_+}\left(\nu J_0 + \frac{\delta/E_c}{\left[\ln(D^*/T_C)\right]^2}\right), \tag{2.32}$$

and with the potential scattering amplitude $V \approx -J/4$. Repeating the argument that led to Eq. (2.15) above, we find that Γ_0 in the r.h.s. of (2.15) is replaced by the renormalized width

$$\Gamma = \pi\nu t^2\big|_{D^*=\delta} = \Gamma_0 + \frac{\pi\delta}{4\big[\ln(\delta/T_C)\big]^2}, \tag{2.33}$$

which translates into the restriction on the allowed values of the addition energy in Eq. (2.32), $E_+ \gg \Gamma$.

2.2.3 Discussion

The exchange amplitude (2.32) determines the value of the Kondo temperature Eq. (1.9). Compared with the Anderson model result $J = (E_C/2E_+)J_0$, see Eq. (2.16), Eq. (2.32) contains an additional contribution, which comes from the renormalization of the tunneling amplitude.

The correction to the tunneling amplitude is of the order of or larger than its bare value if $\gamma_0 \ln(D^*/T_C) \lesssim 1$, see Eq. (2.28). With γ_0 and T_C given in Eq. (2.27), we arrive at the condition

$$D^* \lesssim E_C\gamma_0 \sim E_C\sqrt{\Gamma_0/\delta}\,. \tag{2.34}$$

In view of Eq. (2.34), the most interesting limit is realized when

$$(\delta/E_C)^2 \ll \Gamma_0/\delta. \tag{2.35}$$

For large lateral quantum dots, the left hand side of Eq. (2.35) is controlled by the size of the dot L, $\delta/E_C \propto 1/L$, see the discussion in Section 1.2.1, while the r.h.s is proportional to the conductance of the dot-lead contact. Experimentally, these quantities can be tuned independently of each other [20, 21, 43, 44, 45]. This allows one to satisfy the inequality (2.35) simultaneously with the condition of the applicability of the tunneling Hamiltonian description $\Gamma_0 \ll \delta$.

The inequality (2.35) is equivalent to

$$\ln(\delta/T_C) \ll \sqrt{\delta/\Gamma_0},$$

and is compatible with the condition that $D \sim \delta$ belongs to the weak coupling regime of the Kondo effect in the charge sector, i.e., $\ln(\delta/T_c) \gg 1$. This in turn ensures that the renormalized level width Γ,

$$\Gamma \approx \delta \frac{\pi/4}{\ln^2(\delta/T_c)} ,$$

see Eq. (2.33), is not only large compared with the bare width Γ_0, but is also small compared with the level spacing δ,

$$\Gamma_0 \ll \Gamma \ll \delta. \tag{2.36}$$

Under the conditions (2.35) and (2.36), Eq. (2.32) shows that

$$\nu J(N_0) \approx \frac{1}{\pi E_C \Delta(N_0)} \times \begin{cases} \Gamma, & \Gamma/E_C \ll \Delta(N_0) \lesssim \delta/E_C \\ \Gamma_0, & \Delta(N_0) \gtrsim \sqrt{\Gamma_0/\delta} \end{cases} , \tag{2.37}$$

where

$$\Delta(N_0) = N^* - N_0 + 1/2 \tag{2.38}$$

is the distance in the dimensionless gate voltage to the charge degeneracy point; in terms of $\Delta(N_0)$, the addition energy is given by $E_+(N_0) = 2E_C\Delta(N_0)$, see Eq. (2.2). The dependences Eq. (2.37) coincide with that in the Anderson model, see Eq. (2.16), except that the two asymptotes correspond to two different Anderson models: one characterized by the bare level width Γ_0, another by the renormalized level width $\Gamma \gg \Gamma_0$.

The crossover between the two asymptotes in Eq. (2.37) is smooth, and is described by

$$\nu J(N_0) \approx \frac{\delta}{4E_C\Delta(N_0)} \frac{1}{\ln^2\big[E_C\Delta(N_0)/T_C\big]}, \quad \delta/E_C \lesssim \Delta(N_0) \lesssim \sqrt{\Gamma_0/\delta}\,, \tag{2.39}$$

see Eq. (2.32).

The dependence of the Kondo temperature on the gate voltage is sketched in Fig. 2.1. In this drawing, we took into account that stretching Eqs. (1.9) and (2.32)

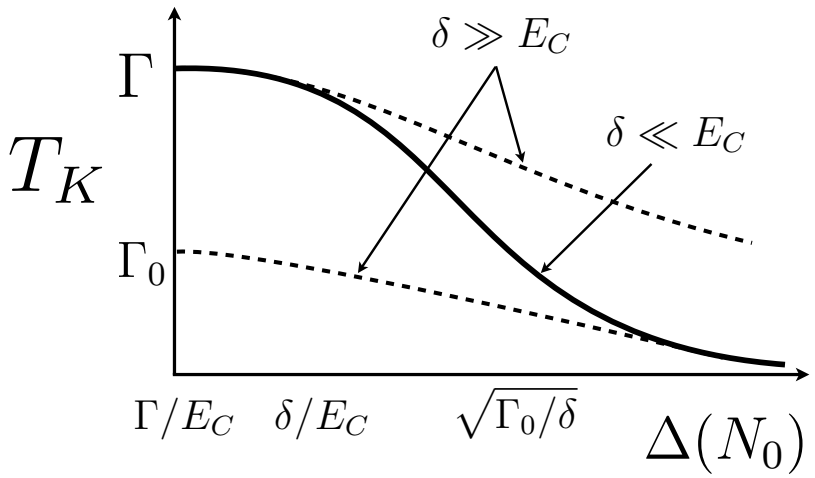

Figure 2.1: Sketch of the dependence of the Kondo temperature T_K on the distance in the dimensionless gate voltage to the charge degeneracy point $\Delta(N_0)$, see Eq. (2.38) The solid line corresponds to a quantum dot ($\delta \ll E_C$) with the bare level width Γ_0. The dashed lines represent single-level Anderson impurity models ($\delta \gg E_C$) with different level widths, Γ and Γ_0.

to the border of the domain of their applicability, $\Delta(N_0) \sim \Gamma/E_C$, gives the estimate $\max\{T_K\} \sim \Gamma$.

Our results show that while the non-monotonic dependence $T_K(N_0)$ prescribed by the Anderson model s qualitatively correct, it is not possible to choose a single parameter characterizing this model (e.g., the tunneling-induced level width) to fit the $T_K(N_0)$ in the entire Coulomb blockade valley with an odd number of electrons.

It should be noted that the dependence $T_K(N_0)$ in quantum dots with almost open contacts [52, 53, 75] is also very different compared with that in the Anderson model. In this case, $(\nu J)^{-1} \sim (E_C/\delta) R \cos^2\left[\pi(N - N^*)\right]$ with $R \ll 1$ [75]. This result applies to dots which are in the mixed valence regime at all values of N_0. Understanding the crossover between the result of [75] and our Eq. (2.32) would require a detailed description of an intermediate regime between the strong and weak Coulomb blockade.

Although the above derivation did not take into account the disorder, our main conclusion remains intact even in the presence of the disorder $T_K(N_0)$ for a quantum dot interpolates between the corresponding dependencies for two different Anderson

models. One of these models is characterized by the bare level width for the Fermi level in the dot, Γ_0, while in the second, Γ_0 is replaced by renormalized width Γ. The renormalization of the width is the result of summing up contributions from a large number ($\sim E_C/\delta \gg 1$) of energy levels in the dot.

APPENDIX A

SCALING FOR THE MULTICHANNEL KONDO MODEL

In this Appendix, we consider the standard anisotropic multichannel Kondo Hamiltonian

$$H = H_0 + \sum_{\alpha m} J_\alpha s^\alpha_m S^\alpha, \quad J_x = J_y = J_\perp \neq J_z \tag{A.1}$$

where

$$H_0 = \sum_{mks} \xi_k \psi^\dagger_{mks} \psi_{nks},$$

$m = 1, ..., M$ labels the channels, independent species of conduction electrons, participating in the exchange, and the local spin densities of conduction electrons are defined as

$$s^\alpha_m = \sum_{kk'ss'} \psi^\dagger_{mks} \frac{\sigma^\alpha_{ss'}}{2} \psi_{mk's'}, \quad \alpha = x, y, z.$$

To proceed, it is convenient to change the notations according to

$$\psi_{mks} = \begin{cases} \psi_{mks}, & |\xi_k| \leq D - \delta D \\ \phi_{mks}, & D - \delta D < |\xi_k| \leq D \end{cases}, \tag{A.2}$$

where ϕ_{nks} represent the electronic states with single particle energies within narrow strips of the width $\delta D \ll D$ near the edges of the band. We write the exchange term in Eq. (A.1) as

$$\sum_{\alpha m} J_\alpha s^\alpha_m S^\alpha = H_{ex} + V, \tag{A.3}$$

where V includes the contributions which do not conserve separately the numbers of ψ and ϕ particles,

$$V = \sum J^\alpha \left(\psi^\dagger_{nks} \frac{\sigma^\alpha_{ss'}}{2} \phi_{nps'} \right) S^\alpha + \text{H.c.}. \tag{A.4}$$

Eq. (A.4) describes transitions between the high-energy states (ϕ) and the rest of the band (ψ). Our goal is to find approximately a unitary transformation $UHU^\dagger$ that

eliminates such processes, similar to the Schrieffer-Wolff transformation in Section 2.1. We seek U in the form

$$U = \exp\left(\sum_{n=1}^{\infty} \Omega_n\right), \quad \Omega_n = -\Omega_n^\dagger \propto J^n, \tag{A.5}$$

and require in addition that the Ω_n, just like V, do not contain terms that commute with both N_ψ and N_ϕ (this requirement removes all ambiguities in the determination of Ω_n). Using the Baker–Hausdorff formula

$$e^A \mathcal{O} e^{-A} = \mathcal{O} + [A, \mathcal{O}] + \frac{1}{2!}[A, [A, \mathcal{O}]] + \frac{1}{3!}[A, [A, [A, \mathcal{O}]]] + ...$$

and collecting terms of the same order in J, we get

$$\begin{aligned} UHU^\dagger &= \sum_{n=0}^{\infty} h^{(n)}, \quad h^{(n)} \propto J^n \\ h^{(0)} &= H_0 \\ h^{(1)} &= H_{ex} + \{V + [\Omega_1, H_0]\} \\ h^{(2)} &= [\Omega_1, V] + \frac{1}{2}[\Omega_1, [\Omega_1, H_0]] + \big\{[\Omega_1, H_{ex}] + [\Omega_2, H_0]\big\}, \end{aligned} \tag{A.6}$$

etc. Requiring ψ-ϕ mixing terms (these terms are placed in curly brackets) to be absent in every order, we get a set of equations

$$\begin{aligned} &[\Omega_1, H_0] + V = 0 \\ &[\Omega_2, H_0] + [\Omega_1, H_{ex}] = 0, \end{aligned} \tag{A.7}$$

etc. Substitution of Eqs. (A.7) into (A.6) yields

$$UHU^\dagger = H_0 + H_{ex} + \frac{1}{2}[\Omega_1, V] + \frac{1}{2}[\Omega_2, V] + O(J^4). \tag{A.8}$$

Eqs. (A.7) are easily solved, resulting in

$$\Omega_1 = \sum \frac{J_\alpha}{\xi_k - \xi_p} \left(\psi^\dagger_{mks} \frac{\sigma^\alpha_{ss'}}{2} \varphi_{mps'}\right) S^\alpha - \text{H.c.} \tag{A.9}$$

$$\begin{aligned} \Omega_2 = &\sum \frac{J_\alpha J_\beta}{(\xi_k - \xi_p)\left(\xi_k - \xi_p + \xi_{k_1} - \xi_{k'_1}\right)} \left[\psi^\dagger_{mks} \frac{\sigma^\alpha_{ss'}}{2} \varphi_{mps'} S^\alpha, \psi^\dagger_{m'k_1s_1} \frac{\sigma^\beta_{s_1s'_1}}{2} \psi_{m'k'_1s'_1} S^\beta\right] \\ &+ \sum \frac{J_\alpha J_\beta}{(\xi_k - \xi_p)\left(\xi_k - \xi_p + \xi_{p_1} - \xi_{p'_1}\right)} \left[\psi^\dagger_{nks} \frac{\sigma^\alpha_{ss'}}{2} \varphi_{nps'} S^\alpha, \phi^\dagger_{n'p_1s_1} \frac{\sigma^\beta_{s_1s'_1}}{2} \phi_{n'p'_1s'_1} S^\beta\right] - \text{H.c.} \end{aligned}$$

So far, no approximations have been made. This stage comes when one tries to actually evaluate the effective Hamiltonian Eq. (A.8). Since our ultimate interest is in the properties of the system at very low energies (much lower, than $D - \delta D$), we can simplify the Hamiltonian even further. First of all, we need to keep only the lowest (not higher than linear) order in $\delta D/D$ contributions. Second, products of the operators will be normal-ordered (for example, we replace $\sum_k A_k \psi^\dagger_{nks}\psi_{nk's}$ by $\sum_k A_k \left\langle \psi^\dagger_{nks}\psi_{nk's}\right\rangle + \sum_k A_k :\psi^\dagger_{nks}\psi_{nk's}:$), and we keep only the most relevant contributions (those that contain products of no more than 2 conduction electron operators). Third, we replace F in the expressions such as $\sum_{ks} F_{ss'}(\xi_k, \xi_{k'}) : \psi^\dagger_{nks}\psi_{nk's'} :$ by its value at the Fermi energy $\xi_k = \xi_{k'} = 0$. To this end, it is sufficient to use the following simplified expression for Ω_2,

$$\Omega_2 \approx \sum \frac{J_\alpha J_\beta s^\beta_m}{(\xi_k - \xi_p)^2}\, \psi^\dagger_{mks} \frac{\sigma^\alpha_{ss'}}{2} \varphi_{mps'} \left[S^\alpha, S^\beta\right] - \text{H.c.}, \tag{A.10}$$

where s^β_m is to be treated as a c-number when calculating, for example, $[\Omega_2, V]$ in Eq. (A.8).

A straightforward (although somewhat lengthy) calculation yields

$$\begin{aligned}
\frac{1}{2}[\Omega_1, V] &\approx \frac{\delta D}{D}\nu \sum_m \left\{ J^2_\perp (s^z_m S^z) + \frac{1}{2} J_z J_\perp (s^+_m S^- + s^-_m S^+) \right\} \qquad (A.11)\\
\frac{1}{2}[\Omega_2, V] &\approx = -\frac{\delta D}{D}\frac{N}{2}\nu^2 \sum_m \left\{ J^2_\perp J_z (s^z_m S^z) + \frac{1}{4}(J^2_z + J^2_\perp) J_\perp (s^+_m S^- + s^-_m S^+) \right\}
\end{aligned}$$

These terms are of the same form as $H_{ex} = \sum_m \left\{ J_z (s^z_m S^z) + \frac{1}{2} J_\perp (s^+_m S^- + s^-_m S^+) \right\}$ in Eq. (A.8). Therefore, apart from the reduced bandwith $D - \delta D$, the only difference between the transformed Hamiltonian (A.8) and the original one (1.2.1) is in the values of the coupling constants [73],

$$J_\alpha \to J_\alpha + \delta J_\alpha$$

with

$$D\frac{\delta J_z}{\delta D} = \nu J^2_\perp - \frac{N}{2}\nu^2 J^2_\perp J_z, \quad D\frac{\delta J_z}{\delta D} J_\perp = \nu J_z J_\perp - \frac{N}{4}\nu^2 \left(J^2_z + J^2_\perp\right) J_\perp. \tag{A.12}$$

Taking here the continuum limit $\delta D/D \to -dD/D = d\zeta$, $\zeta = \ln(D_0/D)$, yields the scaling equations [73]

$$\frac{dJ_z}{d\zeta} = \nu J_\perp^2 - \frac{N}{2}\nu^2 J_\perp^2 J_z, \tag{A.13}$$

$$\frac{dJ_\perp}{d\zeta} = \nu J_z J_\perp - \frac{N}{4}\nu^2 \left(J_z^2 + J_\perp^2\right) J_\perp \,. \tag{A.14}$$

Eqs. (A.13) and (A.14) describe the renormalization of the coupling constants of the Hamiltonian (A.1) with the lowering of the bandwidth. Since we are ultimately interested in physical observables such as the impurity spin operator, the unitary transformation applied to the Hamiltonian should be applied to the operators corresponding to the observable quantities as well.

Of particular interest is the impurity spin operator S^α. Unlike the transformed Hamiltonian, $US^\alpha U^\dagger$ contains terms that mix ψ and ϕ states. These terms, however, do not contribute to the physical quantities such as susceptibility etc., since corresponding processes involve a large ($\sim D$) energy transfer. Therefore, these terms can be neglected as long as $D \gg B, T$, etc. (Note that the scaling Eqs. (A.13), (A.14) are also valid only in this limit.) With this approximation,

$$US^\alpha U^\dagger = S^\alpha + \frac{1}{2}\big[\Omega_1, [\Omega_1, S^\alpha]\big] + O(J^3). \tag{A.15}$$

Keeping only the least fluctuating terms in $[\Omega_1, [\Omega_1, S^\alpha]]$, we find

$$US^\alpha U^\dagger = \left\{1 - \frac{\delta D}{D}\frac{M}{4}\sum_{\beta\neq\alpha}(\nu J_\beta)^2\right\} S^\alpha. \tag{A.16}$$

This can also be written as

$$U(\mu_\alpha S^\alpha)U^\dagger = (\mu_\alpha + \delta\mu_\alpha)\, S^z, \tag{A.17}$$

and interpreted as a renormalization of μ_α (with the initial condition $\mu_\alpha = 1$),

$$D\frac{\delta\mu_\alpha}{\delta D} = -\frac{M}{4}\sum_{\beta\neq\alpha}(\nu J_\beta)^2\mu_\alpha. \tag{A.18}$$

Taking the continuum limit in (A.18), and setting $J_x = J_y = J_\perp$, one obtains

$$\frac{d\mu_z}{d\zeta} = -\frac{M}{2}(\nu J_\perp)^2 \mu_z \,, \tag{A.19}$$

$$\frac{d\mu_\perp}{d\zeta} = -\frac{M}{4}\left[(\nu J_z)^2 + (\nu J_\perp)^2\right] \mu_\perp \,. \tag{A.20}$$

A.1 Solution of the scaling equations

Upon introducing dimensionless coupling constants $I_\alpha = \nu J_\alpha$, Eqs. (A.13), (A.14), and (A.19) can be written as

$$\frac{dI_z}{d\zeta} = I_\perp^2 - \frac{M}{2} I_\perp^2 I_z, \tag{A.21}$$

$$\frac{dI_\perp}{d\zeta} = I_z I_\perp - \frac{M}{4}\left(I_z^2 + I_\perp^2\right) I_\perp, \tag{A.22}$$

$$\frac{d\mu}{d\zeta} = -\frac{M}{2} I_\perp^2 \mu, \tag{A.23}$$

where $\mu \equiv \mu_z$. It is easy to check that the quantities

$$A = \frac{I_\perp^2 - I_z^2}{1 - \frac{M}{2} I_z} \,, \qquad B = \frac{\mu}{1 - \frac{M}{2} I_z} \tag{A.24}$$

remain invariant under the RG flow: $dA/d\zeta = dB/d\zeta = 0$.

A.1.1 Isotropic limit

In the $SU(2)$ invariant case $J_z = J_\perp = J$, and Eqs. (A.21) and (A.22) reduce to a single equation for $I = \nu J$,

$$dI/d\zeta = I^2 - (M/2) I^3. \tag{A.25}$$

By construction, this equation is applicable in the weak coupling regime $I \ll 1$. Accordingly, for $M \sim 1$, the cubic term in the r.h.s. is small, and one can write

$$\frac{dI}{I^2 - (M/2) I^3} \approx dI \left(\frac{1}{I^2} + \frac{M}{2I}\right) = d\zeta,$$

which gives

$$I(\zeta) \approx (\zeta_K - \zeta)^{-1}, \quad \zeta_K = 1/I(0) + (M/2) \ln\big[1/I(0)\big]. \tag{A.26}$$

By definition, $\zeta_K = \ln(D_0/T_K)$, and Eq. (A.26) reduces to

$$\nu J(D) = \left[\ln(D/T_K)\right]^{-1} \tag{A.27}$$

with

$$T_K \simeq D_0(\nu J)^{M/2} \exp(-1/\nu J), \tag{A.28}$$

where J is the bare value of the exchange constant. In the single channel case ($M = 1$) Eq. (A.28) coincides with Eq. (1.9).

A.1.2 Strongly anisotropic limit

Here we consider Eqs. (A.21)-(A.23) for $M \sim 1$ subject to the initial conditions

$$I_z(0) = 1 - \mu(0) = 0, \quad I_\perp(0) = I_0 \neq 0. \tag{A.29}$$

In this case, Eqs. (A.24) yield

$$I_\perp^2(\zeta) - I_z^2(\zeta) = I_0^2\mu(\zeta), \quad \mu(\zeta) = 1 - (M/2)I_z(\zeta) \tag{A.30}$$

By excluding $I_\perp$ from Eq. (A.23) with the help of Eq. (A.30), we obtain an equation for $\eta = 1 - \mu$,

$$\frac{d\eta}{d\zeta} = \frac{MI_0^2}{2}(1-\eta)^2 + \frac{2}{M}\eta^2(1-\eta), \quad \eta(0) = 0. \tag{A.31}$$

Eq. (A.31) is applicable for small η. As in the isotropic case above, the role of higher-order terms in the r.h.s. is to produce a sub-leading logarithmic correction to T_K. To lowest order in η, Eq. (A.31) reduces to

$$\frac{d\eta}{d\zeta} \approx \frac{MI_0^2}{2} + \frac{2}{M}\eta^2. \tag{A.32}$$

Solution of this equation reads [73]

$$\eta(\zeta) = \frac{MI_0}{2}\tan(I_0\zeta). \tag{A.33}$$

At $\zeta \to \pi/2I_0$ the argument of the tangent in (A.33) approaches $\pi/2$, and $\eta(\zeta)$ diverges as

$$\eta(\zeta) \approx \frac{M/2}{\zeta_K - \zeta}, \quad \zeta_K \approx \pi/2I_0. \tag{A.34}$$

Similar to the isotropic case above, taking into account the cubic term in the r.h.s. of Eq. (A.31) produces a subleading logarithmic correction to ζ_K. Consider ζ in the range

$$\zeta_0 \lesssim \zeta \ll \zeta_K$$

with ζ_0 choosen so that $\eta_0 = \eta(\zeta_0) \sim I_0 \ll 1$. In this so-called scaling limit, Eq. (A.31) reduces to

$$\frac{d\eta}{d\zeta} \approx \frac{2}{M}\,\eta^2(1-\eta),$$

which yields Eq. (A.34) with

$$\zeta_K = \frac{M}{2}\big(1/\eta_0 - \ln\eta_0\big)$$

Comparison with ζ_K given in Eq. (A.34) shows that, apart from the logaritmic correction, the two expressions coincide for $\eta_0 = MI_0/\pi \ll 1$,

$$\zeta_K = \pi/2I_0 + (M/2)\ln(1/I_0) = \ln(D_0/T_K). \tag{A.35}$$

This then yields the Kondo temperature

$$T_K \simeq D_0 I_0^{M/2} \exp(-\pi/2I_0). \tag{A.36}$$

Finally, using Eqs. (A.30) and (A.34), we write explicitly solutions of the RG equations (A.21)-(A.23) in the scaling limit,

$$I_z(D) = \frac{1}{\ln(D/T_K)}\,, \tag{A.37}$$

$$I_\perp^2(D) = I_\perp^2(D_0) + \frac{1}{\big[\ln(D/T_K)\big]^2}\,, \tag{A.38}$$

$$\mu(D) = 1 - \frac{1}{\ln(D/T_K)}\,. \tag{A.39}$$

APPENDIX B

DISORDER IN A QUANTUM DOT

In a quantum dot system, the study of the mesoscopic fluctuations of the Kondo temperature has been reported in Kaul *et al.* [76] within the framework of a single-level impurity. However, the mean level spacing δ of a quantum dot has not been of interest until now (see Chap. 2 in details), and this is the motivation of this chapter.

B.1 Introduction

Deviations from an ideal shape of a quantum dot, fluctuations in the quasiparticle and the level spacing due to the gate in transport experiments cause the Kondo temperature to show variations in measurement [77].

The effects of the disorder are already observed in transport experiments in the Coulomb blockade regime [78, 79, 80]. For instance, the statistics of the Coulomb blockade such as spacing between two neighboring peaks, heights of peaks, and the correlation functions were extensively studied both theoretically and experimentally.

In addition, mesoscopic fluctuations of the Kondo temperature in the conventional Kondo effect is also reported with help of the Random Matrix Theory (RMT) [76, 81, 82, 83, 84]. Remembering the effects of the mean level spacing δ in Chap. 2, one would expect that δ affects mesoscopic fluctuations. It turns that δ is substantial, and leads to the analytic form of the probability density of the Kondo temperature $P(T_K)$ even in the presence of the disorder.

B.2 Fluctuation in tunneling amplitudes

The Hamiltonian under consideration is expressed with tunneling amplitudes t_n depending on the dot level n. The tunneling Hamiltonian becomes

$$H_t = \sum_{kn\sigma} (t_n c^\dagger_{k\sigma} d_{n\sigma} + \text{H.c.}). \tag{B.1}$$

The RG correction to each tunneling amplitude t_n in Eq. (B.1) due to the disorder effects is given by a quadratic form of the integrated-out tunneling amplitudes t_p [73].

$$\delta t_n = \frac{1}{D} \sum_{|\varepsilon_p| \in \delta D} t_p^2, \tag{B.2}$$

where $D - \delta D < |\varepsilon_p| < D$. All levels in a dot except a d_0 level at the Fermi level are integrated out as a result of RG, during which the eliminated high energy terms are absorbed into and reflected on, as in Eq. (B.2), the renormalized tunneling amplitude $t'_0 = t_0 + \delta t_0$. Therefore, one gets

$$H_t = \sum_{k\sigma} (t'_0 c^\dagger_{k\sigma} d_{0\sigma} + \text{H.c.}). \tag{B.3}$$

The effective low energy Hamiltonian of a quantum dot is (here, omitting the irrelevant terms in the Hamiltonian)

$$H_{\text{eff}} = \sum_{k,\sigma} (t'_0 c^\dagger_{k\sigma} d_{0\sigma} + \text{H.c.}) + E_c (N - N_0)^2. \tag{B.4}$$

The Schrieffer-Wolff transformation [27] and the use of $SU(2)$ identity relation

$$2\delta_{\sigma_1\sigma_2}\delta_{\sigma'_1\sigma'_2} = \delta_{\sigma_1\sigma'_1}\delta_{\sigma'_2\sigma_2} + \sigma_{\sigma_1\sigma'_1} \cdot \sigma_{\sigma'_2\sigma'_2} \tag{B.5}$$

reduces the effective Hamiltonian to the form of the Kondo model

$$H_K = H_0 + J\mathbf{s} \cdot \mathbf{S}, \tag{B.6}$$

with the spin density of itinerant electrons $\mathbf{s} = c^\dagger_{k\sigma_1} \frac{\vec{\sigma}_{\sigma_1\sigma'_1}}{2} c_{k'\sigma'_1}$ and the dot spin $\mathbf{S} = d^\dagger_{0\sigma_2} \frac{\vec{\sigma}_{\sigma_2\sigma'_2}}{2} d_{0\sigma'_2}$. The anisotropic exchange constant is

$$J = \frac{4t'^2_0}{\min\{E_\pm\}} \tag{B.7}$$

with the renormalized t_0' instead of a bare t_0. As usual, the energy cost is $E_\pm = E_{|N\pm1\rangle} - E_{|N\rangle}$ in the dot.

B.3 Random Matrix Theory

According to random matrix theory, the intensity of tunneling amplitude t_n^2 follows one of the random matrix ensemble, which is gamma distributions, with a breed-number (α, β) reflecting the symmetry in systems [85, 86]

$$P(x) = \frac{1}{\beta^\alpha \Gamma(\alpha)} x^{\alpha-1} e^{-\frac{x}{\beta}}. \tag{B.8}$$

Types of random matrix ensembles, in accordance with its symmetry are the Porter-Thomas distributions (Gaussian Orthogonal Ensemble) for $(\alpha, \beta) = (1/2, 1)$ and the Gaussian Unitary Ensemble for $(\alpha, \beta) = (1, 1)$, respectively. [85]

As a result, the probability density of intensity t_n^2 is given with proper normalization as

$$P(t_n^2) = \frac{1}{\beta^\alpha \Gamma(\alpha)} \frac{t_n^{2\,\alpha-1}}{\overline{t_n^2}^\alpha} e^{-\frac{t_n^2}{\beta \overline{t_n^2}}} \tag{B.9}$$

with the first moment of $x = t_n^2$

$$\overline{x} \;=\; \alpha\beta\overline{t_n^2}$$

and the second moment

$$\overline{x^2} \;=\; \alpha(\alpha+1)\beta^2\overline{t_n^2}^2.$$

B.4 Consequences of mesoscopic fluctuations

Familiarized with the random matrix theory, one is ready to delve into the mesoscopic fluctuations in the dot. We first begin inspecting the middle of the Coulomb blockade valleys, and then switch our interest to the mixed valence regions by tuning the gate voltage, which affects the high energy cut-off of RG in different regions (see Table B.1),

$$D_c(N_0) = \max\{E_\pm(N_0), \delta\}. \tag{B.10}$$

Table B.1: A table of high energy cut-off D of renormalization group in different regions over the gate voltage.

Gate voltage V_g	cut-off D
In the middle of the Coulomb valleys	$E_{+(-)}$
In the intermediate regions	$\max\{\delta, E_{+(-)}\}$
In the vicinity of the mixed valence regions	δ

B.4.1 In the Coulomb blockade valleys

In the middle of the Coulomb blockade valleys, the contribution of higher level states to the zeroth level of a quantum dot at the Fermi level is small due to the high energy cut-off determined by an energy scale of relevance

$$E_{\pm} \approx E_c \gg \delta. \tag{B.11}$$

Let the gate voltage be tuned at $N_0 \approx N^* =$ odd-integer, so that $D_c \approx E_+$. At this gate, where RG runs from D_0 through E_+, Eq. (B.2) becomes

$$\delta t_0 \approx \frac{t_p^2}{D_0}. \tag{B.12}$$

Thus, the mesoscopic fluctuations as a result of RG are

$$t_{\text{eff}} = t_0 + \delta t_0 \approx t_0. \tag{B.13}$$

In other words, the single level contribution dominates the fluctuations, and the result of this fluctuation is expressed as the Porter-Thomas distribution as introduced.

$$P(x) = \frac{1}{\sqrt{2\pi x}} e^{-x}, \tag{B.14}$$

where $x = t_0^2$. In the Coulomb valleys, the exchange interaction also follows the Porter-Thomas distribution since

$$\nu J \approx \nu J_0 = 4\nu t_0^2 / E_c. \tag{B.15}$$

This is quite a consistent and complementary result with earlier work [76], which dealt with the Anderson impurity model, and hence fluctuations of the single level at the Fermi level likely in the middle of the Coulomb valleys here.

B.4.2 Near the mixed-valence regions

The fluctuation is surprisingly suppressed when approaching the mixed-valence region due to many uncorrelated levels in the dot, which are integrated-out during RGs.

The high energy cut-off of RG is now near the mixed-valence regions

$$D_c = \delta. \tag{B.16}$$

About $2D_0/\delta$ (here, $\sim 2E_c/\delta$) number of levels, which are eliminated during RG, contribute to the d_0 level tunneling amplitude t_0 in $t_0' = t_0 + \delta t_0$, and this contribution is greater than the first term, so $t_0' \approx \delta t_0$. This number of eliminated levels is sufficient to apply the central limit theorem to the systems, as often is the case in a large quantum dot. One thus gets the Gaussian distribution due to the mesoscopic fluctuations

$$P(D_0\delta t_0) = \frac{1}{\sqrt{4\pi D_0 \alpha\beta^2(\overline{t_n^2})^2/\delta}} e^{-\frac{\left(D_0\delta t - 2D_0\alpha\beta\overline{t_n^2}/\delta\right)^2}{4D_0\alpha\beta^2(\overline{t_n^2})^2/\delta}} \tag{B.17}$$

with a bare energy bandwidth $D_0 \sim E_c$ (Recall, any t_n^2 follows one of the random matrix ensemble, though.)

This translates into the mesoscopic fluctuations in the Kondo temperature by changing variables in Eq. (B.17) to the Kondo temperature T_K from t_0'

$$t_0' = \frac{1}{2}\sqrt{\frac{E_+}{\nu_c}}\left(\ln\frac{E_+}{T_K}\right)^{-\frac{1}{2}}, \tag{B.18}$$

and one gets

$$\frac{dt_0'}{dT_K} = \frac{1}{4}\sqrt{\frac{E_+}{\nu}}\left(T_K \ln\frac{E_+}{T_K}\right)^{-\frac{3}{2}}. \tag{B.19}$$

It is also shown that T_K is well bounded (see Chap. 2),

$$T_K^{\min} \lesssim T_K \lesssim \Gamma. \tag{B.20}$$

Then, with the help of the probability relation [87]

$$P(T_K)dT_K = P(t_0')dt_0',$$

the probability density $P(T_K)$ is calculated from Eqs. (B.17)-(B.19) with proper normalization, which results in a log-normal distribution [86, 88]

$$P(T_K) = \frac{\mathcal{N}}{T_K} \ln^{-\frac{3}{2}}\left(\frac{E_+}{T_K}\right) \mathrm{Exp}\left[-\frac{\left(E_c\sqrt{E_+/4\nu \ln(E_+/T_K)} - E_c t_0 - E_c\alpha\beta\overline{t_p^2}/\delta\right)^2}{2E_c\alpha\beta^2\overline{t_p^2}^2/\delta}\right] \tag{B.21}$$

with the normalization coefficient $\mathcal{N}$ given by

$$\mathcal{N} = \sqrt{\frac{E_c E_+ \delta}{32\pi\nu\alpha\beta^2\overline{t_n^2}^2}}\left[1 + \mathrm{Erf}\left(\frac{E_c t_0 + E_c\alpha\beta\overline{t_n^2}/\delta}{\sqrt{2E_c\alpha\beta^2\overline{t_n^2}^2/\delta}}\right)\right]^{-1}, \tag{B.22}$$

where $\mathrm{Erf}(x)$ is the error function. We did normalize the probability above approximately (by extending the lower limit and upper limit of the integration) without the introduction of any significant error in the calculation,

$$\int_{T_K^{\min}}^{E_+} P(T_K) dT_K \sim \int_0^{\infty} \frac{1}{\chi^{3/2}} e^{-\frac{1}{2\sigma^2}\left(A/\sqrt{\chi}-B\right)^2} d\chi \tag{B.23}$$

with $\chi = \ln(E_+/T_K)$.

REFERENCES

[1] M. A. Kastner. The single electron transistor and artificial atoms. *Ann. Phys.(Leipzig)*, 9(1):885–894, 2000.

[2] L. P. Kouwenhoven, D. G. Austing, and S Tarucha. Few-electron quantum dots. *Reports on Progress in Physics*, 64(6):701–736, 2001.

[3] T. A. Costi, A. C. Hewson, and V. Zlatic. Transport coefficients of the anderson model via the numerical renormalization group. *Journal of Physics: Condensed Matter*, 6(13):2519–2558, 1994.

[4] D. Goldhaber-Gordon, H. Shtrikman, D. Mahalu, D. Abusch-Magder, U. Meirav, and M. A. Kastner. Kondo effect in a single-electron transistor. *Nature*, 391 (6663):156–159, 1998.

[5] S. M. Cronenwett, T. H. Oosterkamp, and L. P. Kouwenhoven. A tunable kondo effect in quantum dots. *Science*, 281(5376):540–544, 1998.

[6] J. Schmid, J. Weis, K. Eberl, and K. von Klitzing. A quantum dot in the limit of strong coupling to reservoirs. *Physica B: Condensed Matter*, 256-258:182–185, 1998.

[7] W. G. van der Wiel, S. De Franceschi, T. Fujisawa, J. M. Elzerman, S. Tarucha, and L. P. Kouwenhoven. The kondo effect in the unitary limit. *Science*, 289 (5487):2105–2108, 2000.

[8] Y. Ji, M. Heiblum, and H. Shtrikman. Transmission phase of a quantum dot with kondo correlation near the unitary limit. *Phys. Rev. Lett.*, 88(7):076601, 2002.

[9] W. G. van der Wiel, S. De Franceschi, J. M. Elzerman, S. Tarucha, L. P. Kouwenhoven, J. Motohisa, F. Nakajima, and T. Fukui. Two-stage kondo effect in a quantum dot at a high magnetic field. *Phys. Rev. Lett.*, 88(12):126803, 2002.

[10] D. M. Zumbühl, C. M. Marcus, M. P. Hanson, and A. C. Gossard. Cotunneling spectroscopy in few-electron quantum dots. *Phys. Rev. Lett.*, 93(25):256801, 2004.

[11] S. Sasaki, S. De Franceschi, J. M. Elzerman, W. G. van der Wiel, M. Eto, S. Tarucha, and L. P. Kouwenhoven. Kondo effect in an integer-spin quantum dot. *Nature*, 405(6788):764–767, 2000.

[12] S. Sasaki, S. Amaha, N. Asakawa, M. Eto, and S. Tarucha. Enhanced kondo effect via tuned orbital degeneracy in a spin 1/2 artificial atom. *Phys. Rev. Lett.*, 93(1):017205, 2004.

[13] J. Nygård, D. H. Cobden, and P. E. Lindelof. Kondo physics in carbon nanotubes. *Nature*, 408(6810):342–346, 2000.

[14] P. Jarillo-Herrero, J. Kong, H. S. J. van der Zant, C. Dekker, L. P. Kouwenhoven, and S. De Franceschi. Orbital kondo effect in carbon nanotubes. *Nature*, 434 (7032):484–488, 2005.

[15] J. Park, A. N. Pasupathy, J. I. Goldsmith, C. Chang, Y. Yaish, J. R. Petta, M. Rinkoski, J. P. Sethna, H. D. Abruna, P. L. McEuen, and D. C. Ralph. Coulomb blockade and the kondo effect in single-atom transistors. *Nature*, 417 (6890):722–725, 2002.

[16] W. Liang, M. P. Shores, M. Bockrath, J. R. Long, and H. Park. Kondo resonance in a single-molecule transistor. *Nature*, 417(6890):725–729, 2002.

[17] L. H. Yu and D. Natelson. The kondo effect in c60 single-molecule transistors. *Nano Letters*, 4(1):79–83, 2004.

[18] D. C. Mattis. Symmetry of ground state in a dilute magnetic metal alloy. *Phys. Rev. Lett.*, 19(26):1478–1481, 1967.

[19] G. Gruner and A. Zawadowski. Magnetic impurities in non-magnetic metals. *Reports on Progress in Physics*, 37(12):1497–1583, 1974.

[20] M. Pustilnik and L. Glazman. Kondo effect in quantum dots. *Journal of Physics: Condensed Matter*, 16(16):R513, 2004.

[21] L. I. Glazman and M. Pustilnik. Course 7 low-temperature transport through a quantum dot. In S. Guron G. Montambaux H. Bouchiat, Y. Gefen and J. Dalibard, editors, *Nanophysics: Coherence and Transport, cole d't de Physique des Houches Session LXXXI*, volume 81 of *Les Houches Summer School Proceedings*, pages 427 – 478. Elsevier, 2005.

[22] M. Pustilnik. Kondo effect in nanostructures. *Phys. Stat. Sol. (a)*, 203(6):1137–1147, 2006.

[23] J. Kondo. Resistance minimum in dilute magnetic alloys. *Progress of Theoretical Physics*, 32(1):37–49, 1964.

[24] W. J. de Haas, J. de Boer, and G. J. van den Berg. The electrical resistance of gold, copper and lead at low temperatures. *Physica*, 1(7-12):1115 – 1124, 1934.

[25] A.C. Hewson. *The Kondo problem to heavy fermions*. Cambridge studies in magnetism. Cambridge University Press, 1997.

[26] P. W. Anderson. Localized magnetic states in metals. *Phys. Rev.*, 124(1):41–53, 1961.

[27] J. R. Schrieffer and P. A. Wolff. Relation between the anderson and kondo hamiltonians. *Phys. Rev.*, 149(2):491–492, 1966.

[28] H. Suhl. Dispersion theory of the kondo effect. *Phys. Rev.*, 138(2A):A515–A523, 1965.

[29] J. Appelbaum. "$s - d$" exchange model of zero-bias tunneling anomalies. *Phys. Rev. Lett.*, 17(2):91–95, 1966.

[30] P. W. Anderson. Localized magnetic states and fermi-surface anomalies in tunneling. *Phys. Rev. Lett.*, 17(2):95–97, 1966.

[31] E. Burstein and S. Lundqvist. *Tunneling phenomena in solids: lectures*. Plenum Press, 1969.

[32] P. W. Anderson. A poor man's derivation of scaling laws for the kondo problem. *Journal of Physics C: Solid State Physics*, 3(12):2436, 1970.

[33] P. W. Anderson, G. Yuval, and D. R. Hamann. Exact results in the kondo problem. ii. scaling theory, qualitatively correct solution, and some new results on one-dimensional classical statistical models. *Phys. Rev. B*, 1(11):4464–4473, 1970.

[34] F. Wegner. Flow-equations for hamiltonians. *Annalen der Physik*, 506(2):77–91, 1994.

[35] J. W. Franz. Flow equations for hamiltonians. *Nuclear Physics B - Proceedings Supplements*, 90:141 – 146, 2000.

[36] S. D. Glazek and K. G. Wilson. Perturbative renormalization group for hamiltonians. *Phys. Rev. D*, 49(8):4214–4218, 1994.

[37] S. D. Glazek and K. G. Wilson. Asymptotic freedom and bound states in hamiltonian dynamics. *Phys. Rev. D*, 57(6):3558–3566, 1998.

[38] K. G. Wilson. The renormalization group: Critical phenomena and the kondo problem. *Rev. Mod. Phys.*, 47(4):773–840, 1975.

[39] A. M. Tsvelick and P. B. Wiegmann. Exact results in the theory of magnetic alloys. *Advances in Physics*, 32:453–713, 1983.

[40] N. Andrei, K. Furuya, and J. H. Lowenstein. Solution of the kondo problem. *Rev. Mod. Phys.*, 55(2):331–402, 1983.

[41] P. Nozières. A "fermi-liquid" description of the kondo problem at low temperatures. *Journal of Low Temperature Physics*, 17:31–42, 1974.

[42] L. Kouwenhoven and L. Glazman. Revival of the kondo effect. *Physics World*, 14:33–38, 2001.

[43] L. L. Sohn, L. P. Kouwenhoven, and G. Schön. *Mesoscopic electron transport*. NATO ASI series: Applied sciences. Kluwer Academic Publishers, 1997.

[44] M. A. Kastner. The single-electron transistor. *Rev. Mod. Phys.*, 64(3):849–858, 1992.

[45] U. Meirav and E. B. Foxman. Single-electron phenomena in semiconductors. *Semiconductor Science and Technology*, 11(3):255, 1996.

[46] I. L. Aleiner, P. W. Brouwer, and L. I. Glazman. Quantum effects in coulomb blockade. *Physics Reports*, 358(5-6):309 – 440, 2002.

[47] I. Giaever and H. R. Zeller. Superconductivity of small tin particles measured by tunneling. *Phys. Rev. Lett.*, 20(26):1504–1507, 1968.

[48] H. R. Zeller and I. Giaever. Tunneling, zero-bias anomalies, and small superconductors. *Phys. Rev.*, 181(2):789–799, 1969.

[49] J. Lambe and R. C. Jaklevic. Charge-quantization studies using a tunnel capacitor. *Phys. Rev. Lett.*, 22(25):1371–1375, 1969.

[50] C. J. Gorter. A possible explanation of the increase of the electrical resistance of thin metal films at low temperatures and small field strengths. *Physica*, 17(8): 777 – 780, 1951.

[51] C. A. Neugebauer and M. B. Webb. Electrical conduction mechanism in ultrathin, evaporated metal films. *Journal of Applied Physics*, 33(1):74–82, 1962.

[52] K. A. Matveev. Coulomb blockade at almost perfect transmission. *Phys. Rev. B*, 51(3):1743–1751, 1995.

[53] A. Furusaki and K. A. Matveev. Theory of strong inelastic cotunneling. *Phys. Rev. B*, 52(23):16676–16695, 1995.

[54] R. I. Shekhter. Zero Anomalies of the Resistance of Tunnel Junctions Containing Metallic Inclusions in the Oxide Layer. *Sov. Phys. JETP*, 36:747, 1973.

[55] I. O. Kulik and R. I. Shekhter. Kinetic Phenomena and Charge Discreteness Effects in Granulated Media. *Sov. Phys. JETP*, 41:308, 1975.

[56] D. V. Averin and K. K. Likharev. Coulomb blockade of single-electron tunneling, and coherent oscillations in small tunnel junctions. *Journal of Low Temperature Physics*, 62:345–373, 1986.

[57] L. I. Glazman and R. I. Shekhter. Coulomb oscillations of the conductance in a laterally confined heterostructure. *Journal of Physics: Condensed Matter*, 1 (33):5811, 1989.

[58] B. L. Altshuler, P. A. Lee, and R. A. Webb. *Mesoscopic phenomena in solids*. Modern problems in condensed matter sciences. North Holland, 1991.

[59] E. Bonet, M. M. Deshmukh, and D. C. Ralph. Solving rate equations for electron tunneling via discrete quantum states. *Phys. Rev. B*, 65(4):045317, 2002.

[60] C. W. J. Beenakker. Theory of coulomb-blockade oscillations in the conductance of a quantum dot. *Phys. Rev. B*, 44(4):1646–1656, 1991.

[61] D. V. Averin, A. N. Korotkov, and K. K. Likharev. Theory of single-electron charging of quantum wells and dots. *Phys. Rev. B*, 44(12):6199–6211, 1991.

[62] D. V. Averin and Yu. V. Nazarov. Virtual electron diffusion during quantum tunneling of the electric charge. *Phys. Rev. Lett.*, 65(19):2446–2449, 1990.

[63] I. L. Aleiner and L. I. Glazman. Mesoscopic fluctuations of elastic cotunneling. *Phys. Rev. Lett.*, 77(10):2057–2060, 1996.

[64] A. F. G. Wyatt. Anomalous densities of states in normal tantalum and niobium. *Phys. Rev. Lett.*, 13(13):401–404, 1964.

[65] R. A. Logan and J. M. Rowell. Conductance anomalies in semiconductor tunnel diodes. *Phys. Rev. Lett.*, 13(13):404–406, 1964.

[66] T. K. Ng and P. A. Lee. On-site coulomb repulsion and resonant tunneling. *Phys. Rev. Lett.*, 61(15):1768–1771, 1988.

[67] R. G. Newton. *Scattering theory of waves and particles*. Dover books on physics. Dover Publications, 2002.

[68] F. D. M. Haldane. Scaling theory of the asymmetric anderson model. *Phys. Rev. Lett.*, 40(6):416–419, 1978.

[69] F. D. M. Haldane. Theory of the atomic limit of the anderson model. i. perturbation expansions re-examined. *Journal of Physics C: Solid State Physics*, 11 (24):5015, 1978.

[70] M. Pustilnik and L. Borda. Phase transition, spin-charge separation, and spin filtering in a quantum dot. *Phys. Rev. B*, 73(20):201301, 2006.

[71] I. Garate and I. Affleck. Kondo temperature in multilevel quantum dots. *Phys. Rev. Lett.*, 106(15):156803, 2011.

[72] S. Nah and M. Pustilnik. Kondo temperature of a quantum dot. *ArXiv e-prints*, 2011.

[73] K. A. Matveev. Quantum fluctuations of metallic particle charge under coulomb blockade conditions. *Sov. Phys. JETP*, 72:892–899, 1991.

[74] M. Pustilnik, Y. Avishai, and K. Kikoin. Quantum dots with even number of electrons: Kondo effect in a finite magnetic field. *Phys. Rev. Lett.*, 84(8):1756–1759, 2000.

[75] L. I. Glazman, F. W. J. Hekking, and A. I. Larkin. Spin-charge separation and the kondo effect in an open quantum dot. *Phys. Rev. Lett.*, 83(9):1830–1833, 1999.

[76] R. K. Kaul, D. Ullmo, and H. U. Baranger. Mesoscopic fluctuations in quantum dots in the kondo regime. *Phys. Rev. B*, 68(16):161305(R), 2003.

[77] I. L. Aleiner and L. I. Glazman. Mesoscopic charge quantization. *Phys. Rev. B*, 57(16):9608–9641, 1998.

[78] S. R. Patel, S. M. Cronenwett, D. R. Stewart, A. G. Huibers, C. M. Marcus, C. I. Duruöz, J. S. Harris, K. Campman, and A. C. Gossard. Statistics of coulomb blockade peak spacings. *Phys. Rev. Lett.*, 80(20):4522–4525, 1998.

[79] R. A. Jalabert, A. D. Stone, and Y. Alhassid. Statistical theory of coulomb blockade oscillations: Quantum chaos in quantum dots. *Phys. Rev. Lett.*, 68 (23):3468–3471, 1992.

[80] U. Sivan, R. Berkovits, Y. Aloni, O. Prus, A. Auerbach, and G. Ben-Yoseph. Mesoscopic fluctuations in the ground state energy of disordered quantum dots. *Phys. Rev. Lett.*, 77(6):1123–1126, 1996.

[81] Y. Alhassid, T. Rupp, A. Kaminski, and L. I. Glazman. Linear conductance in coulomb-blockade quantum dots in the presence of interactions and spin. *Phys. Rev. B*, 69(11):115331, 2004.

[82] A. Kaminski, I. L. Aleiner, and L. I. Glazman. Mesoscopic charge fluctuations in the coulomb blockade regime. *Phys. Rev. Lett.*, 81(3):685–688, 1998.

[83] R. K. Kaul, D. Ullmo, S. Chandrasekharan, and H. U. Baranger. Mesoscopic kondo problem. *EPL (Europhysics Letters)*, 71(6):973, 2005.

[84] S. Kettemann and E. R. Mucciolo. Disorder-quenched kondo effect in mesoscopic electronic systems. *Phys. Rev. B*, 75(18):184407, 2007.

[85] F. Haake. *Quantum Signatures of Chaos*. Springer-Verlag, 2001.

[86] G. Arfken and H. Weber. *Mathematical Methods for Physicists*. Academic Press, 1995.

[87] W. H. Press, B. P. Flannery, S. A. Teukolsky, and W. T. Vetterling. *Numerical Recipes in C: The Art of Scientific Computing*. Cambridge University Press, 1992.

[88] I. S. Gradshteyn and I. M. Ryzhik. *Table of integrals, series, and products*. Academic Press, 1980.

VITA

Seungjoo Nah was raised in Gwangju, Korea, where he first met his wife Doah Kim in October 1995. He went to Seoul National University (SNU), Seoul, Korea, in March 1996, and earned a B.S. in physics in February 2000. He subsequently continued his research on optics and eventually developed an interest in quantum computing during his M.S. under the supervision of Profs. Jai-Hyung Lee and Joon-Sung Chang at SNU. He enlisted in the R.O.K. Navy in March 2002 and was commissioned an Ensign in June 2002. In July 2005, after finishing three year's duty and hence being discharged from the Navy, he came to the U.S. to further pursue his goal at Georgia Tech following Prof. Choonkyu Lee's advice - to become *a physicist*. He has worked on mesoscopic physics under Prof. Michael Pustilnik since May 2006.